

DEPENDENCE OF BORON *AND* SODIUM IN FLUE GAS FROM
A BOROSILICATE GLASS MELTING FURNACE ON
CONDITIONS IN THE CAUSTIC SPRAY TOWER
AND ELECTROSTATIC PRECIPITATOR

Peter M. Walsh, Howard A. Johnsen, David K. Ottesen, and Shane M. Sickafoose

Sandia National Laboratories
Livermore, California

Report prepared for the
CertainTeed Corporation Insulation Group
Blue Bell, Pennsylvania and Chowchilla, California
and the
Glass Manufacturing Industry Council
Westerville, Ohio

Project supported by the
Glass Manufacturing Industry Council
and the
U.S. Department of Energy, Office of Industrial Technologies,
Industries of the Future Glass Team
under the
Glass - Project Laboratory User Services (G+) Program

August 27, 2002

CONTENTS

<u>Section</u>	<u>Page</u>
List of Tables	iv
List of Figures	v
Acknowledgments	viii
Introduction	1
Experimental Measurements and Data Analysis	2
Test Site, Sampling Location, Program, and Procedure	2
Process Conditions	2
Caustic Soda Solution	4
Measurement of Boron and Sodium	5
Determination of Gas Flow Rate in the Flue	5
Electrostatic Precipitator Dust	6
Experimental Results	7
Boron	7
Time Dependence	7
Effect of Temperature	12
Effect of Sodium Feed Rate	14
Effect of Caustic Soda Atomizing Air Pressure	14
Comparison with the Boron Measurements in August 2000	17
Sodium	18
Time Dependence	18
Effect of Temperature	20
Effect of Sodium Feed Rate	20
Effect of Caustic Soda Atomizing Air Pressure	20
Equilibrium Model Calculations	24
Discussion	35
Temperature	35
Sodium Addition	35
Atomizing Air Pressure	39
Water Vapor	39
Collection Efficiency for Sodium	40
Remaining Questions	40

CONTENTS (continued)

<u>Section</u>	<u>Page</u>
Summary, Conclusions, and Recommendations	41
Summary and Conclusions	41
Recommendations	44
Nomenclature	47
References	48
Appendices	
A. Tables of conditions during the runs.	A1
B. Analysis of the natural gas.	B1
C. Plots of process conditions.	C1
D. Analyses of caustic soda samples and calibration curves.	D1
E. Computer code for calculation of the flue gas flow rate.	E1
F. Analysis of dust from the electrostatic precipitator.	F1
G. Review of some data from August 2000.	G1

LIST OF TABLES

<u>Table</u>	<u>Page</u>
1. Run Conditions, Boron and Sodium Concentrations, and Boron and Sodium Mass Flow Rates at the Electrostatic Precipitator Outlet.	8
A1. Run Dates and Times, Ambient Conditions, Oxygen Purity, Natural Gas Properties, and Oxygen and Gas Flow Rates.	A2
A2. Furnace Conditions, Quench Water Flow, Temperature in Horizontal Flue, Caustic Soda Properties, and Atomizing Air Pressure.	A5
A3. Electrostatic Precipitator Temperatures, Conditions at the Sampling Point, Flue Gas Flow, Opacity, and NO _x	A8

LIST OF FIGURES

<u>Figure</u>	<u>Page</u>
1. Mass flow rates of boron at the outlet from the electrostatic precipitator versus the time of day.	11
2. Mass flow rates of boron at the outlet from the electrostatic precipitator versus temperature at the outlet from the electrostatic precipitator.	13
3. Mass flow rates of boron at the outlet from the electrostatic precipitator versus the feed rate of sodium to the caustic soda spray tower.	15
4. Mass flow rates of boron at the outlet from the electrostatic precipitator versus the pressure of the caustic soda atomizing air.	16
5. Mass flow rates of sodium at the outlet from the electrostatic precipitator versus the time of day.	19
6. Mass flow rates of sodium at the outlet from the electrostatic precipitator versus temperature at the outlet from the electrostatic precipitator.	21
7. Mass flow rates of sodium at the outlet from the electrostatic precipitator versus the feed rate of sodium to the caustic soda spray tower.	22
8. Mass flow rates of sodium at the outlet from the electrostatic precipitator versus the pressure of the caustic soda atomizing air.	23
9. Results of calculations using the NASA Chemical Equilibrium with Applications Code and thermodynamic property database at an alkali to boron-plus-sulfur mole ratio of 0.96.	27
10. Results of calculations of equilibrium chemical composition in the electrostatic precipitator at an alkali to boron-plus-sulfur ratio of 0.98.	28
11. Results of calculations of equilibrium chemical composition in the electrostatic precipitator at an alkali to boron-plus-sulfur ratio of 1.00.	29
12. Results of calculations of equilibrium chemical composition in the electrostatic precipitator at an alkali to boron-plus-sulfur ratio of 1.094, the value indicated by chemical analysis of the precipitator dust.	32

LIST OF FIGURES (continued)

<u>Figure</u>	<u>Page</u>
13. Calculated mole fractions of orthoboric acid vapor as functions of temperature.	33
14. Relationship between orthoboric acid vapor concentration and alkali to boron-plus-sulfur ratio at the precipitator outlet temperature of 485 °F.	34
15. Comparison of the measurements of boron flow rate at the precipitator outlet with the calculations of boron expected at equilibrium using the NASA CEA Code, shown as functions of temperature.	36
16. Comparison of the measurements of boron flow rate at the precipitator outlet with the calculations of boron expected at equilibrium using the NASA CEA Code, shown as functions of the sodium feed rate to the caustic spray tower.	37
C1. Temperature in the furnace, horizontal flue, electrostatic precipitator inlet and outlet, and ambient versus the time of day.	C2
C2. Furnace temperature, oxygen flow rate, natural gas flow rate, oxygen to natural gas ratio, flue gas quench water flow rate, and NO _x flow rate in the stack versus the time of day.	C3
C3. Stack gas opacity versus the time of day.	C4
C4. Boron concentration in the flue gas at the outlet from the electrostatic precipitator versus stack gas opacity.	C5
C5. Temperature at the inlet to the electrostatic precipitator versus the flow rate of caustic soda solution to the spray tower.	C6
C6. Temperature difference from the inlet to the outlet of the electrostatic precipitator versus the difference between the inlet temperature and ambient temperature.	C7
D1. Specific gravity of samples of the caustic soda solution taken from the delivery line versus the indicated density readings in the control room.	D6
D2. Mass fraction of NaOH determined by analysis of the caustic soda samples taken from the delivery line versus the indicated density readings in the control room.	D7

LIST OF FIGURES (continued)

<u>Figure</u>	<u>Page</u>
D3. Density of caustic soda solutions versus mass fraction of NaOH at 86 °F.	D8
D4. Calibration of the gauge used to measure the pressure of the caustic soda atomizing air.	D9
D5. Relationship between the volumetric flow rate of flue gas and the static pressure in the duct.	D10
G1. Comparison of the sequence of August 31, 2000, measurements of boron at the electrostatic precipitator outlet with the sequence of oxygen-to-gas ratios. . .	G2
G2. August 31, 2000, measurements of boron at the electrostatic precipitator outlet versus electrostatic precipitator outlet temperature.	G3

ACKNOWLEDGMENTS

The work described in this report was supported by the CertainTeed Corporation Insulation Group, the Glass Manufacturing Industry Council, and the U.S Department of Energy, Office of Industrial Technologies, Industries of the Future Glass Team, under the Glass Project Laboratory User Services (G+) program. The authors thank the CertainTeed Corporation, the Glass Manufacturing Industry Council, and the Department of Energy for their support of the investigation. We are indebted to Eric Schramm, Plant Manager, and Dave Kawano, Hot End Manager, for providing access to the CertainTeed Insulation Group's Chowchilla, California, Plant and the equipment and assistance needed to make the measurements. Thanks to Terry L. Berg, Jeffrey T. Curtin, and Markus H. Stahl for their close collaboration during all stages of the planning and execution of the tests, and to Mike Harris, Lonnie Herring, and Dean Bailey for their work on the set-up and maintenance of the equipment for the measurements. We are also grateful to Terry Berg for his help with the measurements of the gas velocity profiles and to Jeff Curtin, Mark Stahl, and Jacob Mu (U.S. Borax) for many valuable discussions.

Interpretation of the data was greatly facilitated by comparison with the results of calculations using the NASA Chemical Equilibrium with Applications Code. The authors thank Bonnie J. McBride of the NASA Glenn Research Center for providing the properties of sodium tetraborate for addition to the thermodynamic database.

INTRODUCTION

The work described in this report continues an investigation of the influence of process and flue gas treatment conditions on the flow rates of boron and sodium in the exhaust from an oxygen/natural-gas-fired borosilicate glass melting furnace. A previous report (Walsh, Johnsen, and Ottesen, 2001) described the results of a study of the effect of the oxygen-to-natural-gas ratio at the burners on the boron and sodium flow rates in the flue downstream from the furnace and at the exit from the electrostatic precipitator. The focus of the present work is on the influence of the caustic soda introduced into the flue gas on the flow rates of boron and sodium leaving the precipitator.

Particulate matter formed from the vapor of boron and sodium species volatilized from molten borosilicate glass (Beerkens and van Limpt, 1998), plus any batch dust, slag droplets, and other particles carried over from the melting furnace can be removed with high efficiency using standard particulate control technology, such as an electrostatic precipitator. However, some boric acids are sufficiently stable in the vapor phase and have partial pressures at the gas temperatures in a precipitator high enough that some boron is able to pass through the precipitator as vapor (Slade, 1996; J. T. Curtin, personal communications, 2000), contributing to particulate matter determined using US EPA Method 5 (Code of Federal Regulations, 1996), especially to the condensable fraction. At the CertainTeed Corporation insulation plant, caustic soda solution (aqueous sodium hydroxide) is injected into the flue gas in a spray tower upstream from the electrostatic precipitator, to promote conversion of boric acid vapors to solid sodium borates (Beerkens and van Limpt, 2001), which are collected by the precipitator with high efficiency. The purpose of the present investigation was to determine the effects of caustic soda and spray tower conditions, in particular the solution concentration, flow rate, and spray quality, on the collection of boron in the electrostatic precipitator, with a view to optimizing the treatment of flue gas.

EXPERIMENTAL MEASUREMENTS AND DATA ANALYSIS

Test Site, Sampling Location, Program, and Procedure

The experiments were conducted at the CertainTeed Corporation Insulation Group's Fiberglass Insulation Plant in Chowchilla, California. The measurement point was downstream from the electrostatic precipitator, between the precipitator and the induced draft fan, through the same sampling port used for measurements downstream from the precipitator a year earlier (Walsh, Johnsen, and Ottesen, 2001). The measurement point was 7.75 in. from the inside wall of the duct, compared with 6.375 in. from the wall during the previous tests.

The equipment was set up during the late morning and afternoon of Friday, August 3, 2001. A single set of measurements of boron and sodium was collected in the early evening that day, followed by traverses of the duct using a Pitot/static probe to determine gas velocity profiles. Measurements of boron and sodium continued during the days of August 4, 5, and 6. The equipment was broken down, packed up, and returned to Livermore on Tuesday, August 7.

The conditions varied intentionally during the tests were the caustic soda flow rate, caustic soda density, and the caustic soda atomizing air pressure. The measurements with variation of caustic soda flow rate and density were done on August 4 and 5; the measurements with variation of atomizing air pressure on August 6. The ambient temperature, which varied through the course of a day, also turned out to be an influential variable.

The procedure was to set the caustic soda flow rate, density, and atomizing air pressure at the desired values, then wait for approximately 30 minutes for the system to reach steady state. Recording the average of the spectra from 1000 laser sparks took slightly under two minutes, so collection and storage of six 1000-shot averages for boron and another six for sodium took approximately 30 minutes. While this was being done another member of the team recorded the process data in the control room, on the caustic soda spray tower, and at the flue. The typical time required for a complete run was 1 hour. A total of 37 runs were done, at the conditions given in Appendix A, Tables A1, A2, and A3.

Process Conditions

Values of the following process variables were recorded during each run: oxygen flowrate, oxygen purity, natural gas flowrate, natural gas heating value and specific gravity, furnace temperature, furnace pressure, flue gas quench water flowrate,

temperature in the horizontal flue, temperatures at the inlet and outlet of the electrostatic precipitator, stack gas opacity (1 and 3 min running averages), and NO_x emission. Properties of the caustic soda and its spray conditions are discussed in the following section. Ambient temperature, relative humidity, and barometric pressure were also noted. The humidity was needed to calculate the flow rate of water vapor entering the system with inleaking air. These data are all listed in Tables A1, A2, and A3. A composite analysis of the natural gas in the pipeline serving the plant during the period from July 31 to August 7, provided by the supplier, is attached as Appendix B.

Most process conditions were similar to those during the tests a year earlier. The pull rate was the same as it had been before and the oxygen-to-natural-gas ratio was 1.86, practically identical to that at the base condition of the previous tests, 1.85. The most significant change was a reduction in the density of the caustic soda solution fed to the spray tower, from an indicated value of 1.09 g/mL in August 2000 to 1.044 g/mL at the time of the present tests in August 2001. The flow rate of the solution during the earlier tests was the same as that at the base condition of the present tests, 1.0 gal/min. Based on the calibration of the density meter, to be described later, and assuming that there was no change in the calibration during the year between the tests, it is estimated that the feed rate of sodium (expressed as the element, Na) in August 2000 was 22.9 lb/hour, compared with a rate of 8.62 lb/h in August 2001.

Plots of the measurements of furnace temperature, gas temperature in the horizontal flue, temperatures at the inlet and outlet of the electrostatic precipitator, and the ambient temperature are shown as a function of the clock time on each day of testing in Appendix C, Figure C1. The furnace and flue gas temperatures are held fixed within very close tolerances by automatic control. The ambient temperature, which will be shown later to be of some importance, follows an expected trajectory with a maximum at about 16:00 hours. The days of August 4, 5, and 6 became progressively warmer. Temperatures at the inlet and outlet of the electrostatic precipitator, which would normally be expected to show a systematic relationship to the ambient temperature, are here confounded with the changes being made to the flow rate of caustic soda to the spray tower during the course of the tests.

The natural gas flow rate to the burners, oxygen-to-gas ratio, quench water flow rate to the flue, and NO_x emissions are compared with the furnace temperatures in Figure C2. None of the conditions upstream from the caustic spray tower, such as the oxygen to natural gas ratio, quench water flow rate, and temperature in the horizontal flue, showed any marked change or periodic behavior over the entire four days of tests. The natural gas flow rate did decrease slightly during the course of each day (by approximately 3% from 8 a.m. to 6 p.m.) and the NO_x emissions showed a slight upward trend (from about 30 lb/h to about 32 lb/h over the same period).

In contrast with the other conditions, the in-stack opacity, shown in Figures C3a (1-minute averages) and C3b (3-minute averages) exhibits a systematic behavior, reproducible from day to day. The 3-minute averages, which are less noisy and therefore more useful (Figure C3b), decrease during the period from 8:30 to about 13:00 hours,

then increase slightly during the remainder of the day. The opacity reading is not a reliable indicator of boron concentration, however, because other streams from the plant are mixed with the flue gas upstream from the stack.

Caustic Soda Solution

The plan for the tests contained three variables related to the caustic soda: density, flow rate, and air pressure at the spray nozzle. The density and flow rate were read from the monitors in the control room and the air pressure from the gauge mounted on the lance at the top of the spray tower. The density was varied by changing the speed of the metering pump in the caustic soda mixing room; the flow rate was changed by the furnace operator in the control room; and the atomizing air pressure was varied using the pressure regulator at the top of the spray tower. Samples of the concentrated (50 wt%) caustic soda from the storage tank and three samples of diluted caustic soda from the tee in the delivery line (near the guard rail on the maintenance platform next to the area where the vertical flue joins the horizontal flue) were collected and analyzed later, with the results shown in Appendix D. For a short time, during runs 21 to 24, no caustic soda was introduced at all, so the corresponding density reading in the control room, when only water was flowing through the system, provides another comparison of the density indicated by the control system with a known value.

The specific gravities at 60/60°F (ratio of the mass of a given volume of the solution at 60°F to the mass of the same volume of water at the same temperature) of the two diluted samples measured by the laboratory, plus the value for water, are plotted versus the density indicated on the monitors in the control room in Appendix D, Figure D1. At low values of the density the indicated reading is considerably higher than the actual specific gravity, but the error decreases with increasing density. The equation with which the indicated values can be corrected is shown in the figure. The laboratory also performed analyses of the samples for the weight percent NaOH, which is a more useful number than the specific gravity for our present purposes. A plot of the mass fraction of NaOH in the diluted caustic soda versus the indicated density is shown in Figure D2. One more piece of information is needed to calculate the mass flow rates of NaOH into the spray tower: the densities of the solutions at the temperature of the flow meter. The temperature was estimated as roughly 30°C (86°F) and the dependence of density on the mass fraction of NaOH at this temperature was obtained from data provided by the Dow Chemical Company (2001). A plot of the Dow data is shown in Figure D3. The procedure for calculating the mass flow rate of Na was, starting with the indicated density, to first determine the mass fraction of NaOH (Figure D2), then the density of the solution (Figure D3). The product of the mass fraction, density, solution flow rate, and the ratio of the atomic weight of Na to the formula weight of NaOH with the appropriate conversion factors for time, volume, and mass gave the feed rate of sodium to the spray tower. The data and results are given in Table A2.

At the conclusion of the tests, the pressure gauge on the caustic soda spray lance was removed and replaced with new one. The gauge used during the tests was calibrated

using a dead weight tester, with the results shown in Figure D4. Both the uncorrected and corrected pressures are given in Table A2.

Measurement of Boron and Sodium

The technique used to measure boron and sodium was laser-induced breakdown spectroscopy (LIBS) or laser spark spectroscopy. In this method a pulsed neodymium-doped yttrium aluminum garnet (Nd:YAG) laser is focused in the gas/particle mixture to be analyzed. The high electric field at the focal point causes electric breakdown and generates a small volume of plasma at extremely high temperature, on the order of 25,000°F. The visual appearance of the plasma is that of a small spark. At such a temperature all particles and droplets are vaporized, all molecules dissociated, and virtually all of the resulting atoms are ionized. As the plasma cools and the electrons and ions recombine and relax toward their ground states, the atoms of each element emit light at characteristic wavelengths. The emission spectrum is resolved using a grating spectrometer and recorded using a charged coupled device (CCD) camera. The delay between the firing of the laser and the collection of the spectrum, and the time interval during which the spectrum is recorded, are chosen to optimize the signal to noise ratio for the elements of interest. Only a small part of the emission spectrum, typically 35 nm wide, was recorded at a time, to increase wavelength resolution. Therefore, boron, whose strongest accessible emission lines are at 250 nm, and sodium, whose strongest lines are at 589 nm, were not measured simultaneously. The laser fires and generates a new spark and new analysis 9 times per second. One thousand individual shots were added together to obtain a high quality spectrum. Typically six of these 1000-shot averages were collected for boron and another six for sodium at each experimental condition. A diagram of the optical system of the LIBS instrument and a photograph of the instrument mounted on the duct downstream from the electrostatic precipitator may be found in the report by Walsh, Johnsen, and Ottesen (2001). Additional information on the LIBS technique and its application to measurements in glass melting furnace flues is provided in the paper by Buckley et al. (2000).

Determination of Gas Flow Rate in the Flue

The LIBS measurements provided the concentrations of boron and sodium in the flue gas, but the mass flow rates of the elements are more useful for interpretation of the data, free from the influence of changes in concentration due simply to changes in the dilution of the elements by fluctuations in the natural gas, oxygen, and quench water flow rates or the intentional changes in caustic soda flow rate, rather than to changes in the performance of the flue gas treatment system. Changes in concentration due to dilution were much less significant than they had been during the previous series of tests, when the oxygen-to-natural-gas ratio was varied, but it was still necessary to account for it, because the effects under study during the present tests were expected to be more subtle.

In the previous tests, because measurements downstream from the electrostatic precipitator were not part of the original test plan, the Pitot/static probe brought to the plant barely reached to the centerline of the 41 in. diameter duct, and a traverse of the

duct to determine the gas velocity profile was not possible. The calculations were done under the assumption of a fully-developed turbulent flow profile at the Reynolds number in the duct.

A longer probe was obtained for the present tests and traverses of the duct were made along two perpendicular paths under the plant's current standard operating condition to determine the average mass flux of flue gas. A point at which the flux was close to the average value was then chosen as a reference location, at which the gas velocity was measured during most runs. The same ratio of gas velocity at the reference point to the average velocity was assumed to apply under all of the conditions studied. The following data, required for the calculation of gas velocity, were recorded during most runs: Pitot/static pressure difference, static pressure in the duct, barometric pressure, and gas temperature at the measurement point. The values are given in Tables A1 and A3. The average molecular weight of the flue gas, also needed for the calculation of gas velocity, was determined by an iterative calculation procedure in which the amount of air in the flue gas was varied until the total volumetric flow rate calculated from the oxygen, natural gas, batch gases, batch fuel oil, quench water, caustic soda feeds, and air, assuming complete combustion, agreed closely with the flow rate calculated from the Pitot/static pressure difference, using the average molecular weight based on the feeds. The computer code used to perform these calculations is attached as Appendix E. The calculated volumetric flow rate during each run is given in Table A3. The total range of variation in flow rate over all runs was only $\pm 3.3\%$ of the average. The typical value is 70% larger than that estimated during the tests of August 2000.

There was a series of runs (no's. 8 through 14) during which the Pitot/static pressure difference was not recorded, because the inclined oil manometer had been blown out. The flow rate of flue gas was estimated for these runs by constructing a plot of flow rate versus the static pressure in the flue for all the other runs, shown in Appendix D, Figure D5, then using the line fit to these data by the method of least squares to estimate the unknown flow rates. These results are listed in Table A3 enclosed in parentheses. Their uncertainty is approximately the range of the points shown in Figure D5, $\pm 0.1 \text{ m}^3/\text{s}$.

Electrostatic Precipitator Dust

A sample was collected from the electrostatic precipitator on the morning of August 4, 2001, and later sent to a lab for analysis. The results are attached as Appendix F. The B_2O_3 , Na_2O , K_2O , and SO_3 contents of the dust were 29.50, 29.78, 5.59, and 22.55 wt%, respectively, compared with 24.8, 35.7, 5.61, and 17 wt%, respectively, a year earlier. The change in composition reflects the decrease in sodium feed to the caustic spray tower between the two tests.

EXPERIMENTAL RESULTS

The values of the key test conditions and the results for boron and sodium are given in Table 1. Both the concentrations, direct from the LIBS measurements, and the mass flow rates of boron and sodium, equal to the product of concentration and the volumetric flow rate of flue gas (from Table A3) are shown, expressed in terms of the masses of the elements, not as their oxides or other chemical combination. The total flow rate of condensable species, assuming, for example, that the form of boron after drying the contents of the back half of the US EPA Method 5 sampling train is metaboric acid, would be found by multiplying the boron mass flow rate by the ratio of the molecular weight of HBO_2 to the atomic weight of boron, $43.82/10.811 = 4.1$. The standard deviations given in Table 1 are those of the values for concentration and flow rate derived from the multiple (usually six) 1000-shot average LIBS intensity measurements. The results for boron, the more abundant of the two elements, will be discussed first, followed by the results for sodium.

Boron

Time Dependence

The mass flow rates of boron in the flue on the four days of testing are shown as a function of the time of day in Figure 1. On the first day of testing, August 3, there was only one run, at about 18:00 hours. The following features of the data are immediately apparent:

1. The data fall into two distinct groups, one having boron flow rates in the range from 0.015-0.3 lb/h and the other having flow rates of roughly 0.4 to 0.5 lb/h. There was an abrupt shift from the lower to the higher boron flow rates at about 14:00 hours on August 5.
2. There is a periodic behavior that is remarkably similar from day to day. The most reproducible feature is a minimum in the boron flow rate in the afternoon, a little before 16:00 hours, coinciding with the peak in ambient temperature (Figure C1).

The abrupt increase in boron flow rate near 14:00 hours on August 5 has been the subject of much discussion and prompted extensive examination of the data. It has not been possible to determine whether the change was associated with the performance of the LIBS equipment or to an actual change in boron concentration in the flue. No change in laser pulse energy, detector sensitivity, optical alignment, calibration, etc. was observed before and after the apparent change in concentration or from the beginning to the end of the tests. A significant increase in the opacity occurred at the same time as the

Table 1.
Run Conditions, Boron and Sodium Concentrations, and Boron and Sodium Mass Flow Rates at the Electrostatic Precipitator Outlet.

Run No.	Date	- Caustic Soda - gpm	lb Na/h	At. Air P, psig ^b	EP Out T, °F	- B Conc., ave.	$\mu\text{g}/\text{m}^3$	- Na Conc., ave.	$\mu\text{g}/\text{m}^3$	--- B Flow, lb/h --- ave.	std. dev.	--- Na Flow, lb/h --- ave.	std. dev.
1 ^a	8/3	1.0	8.32	59.3	469	4039	86	7.3	3.8	0.2687	0.0057	0.00048	0.00025
2 ^a	8/4	1.0	8.91	60.1	452	4712	113	1.9	1.1	0.3108	0.0074	0.00012	0.00007
3	8/4	1.0	14.37	60.3	454	3241	64	1.9	0.8	0.2117	0.0042	0.00013	0.00005
4	8/4	1.0	19.22	60.3	455	3193	100	1.7	2.8	0.2105	0.0066	0.00011	0.00018
5	8/4	1.0	0.25	60.3	458	3801	104	3.6	1.8	0.2511	0.0069	0.00023	0.00012
6	8/4	1.25	0.31	60.3	459	4140	42	0.008	0.019	0.2742	0.0028	6×10^{-7}	12×10^{-7}
7	8/4	1.25	8.19	60.3	456	3757	59	4.4	1.6	0.2494	0.0039	0.00029	0.00010
8	8/4	1.25	12.64	(60.3)	454	3244	51	4.0	1.8	0.2150	0.0034	0.00026	0.00012
9	8/4	1.25	19.89	60.3	455	2888	51	2.5	1.8	0.1944	0.0035	0.00017	0.00012
10	8/4	0.75	20.75	60.3	459	2818	50	2.1	1.4	0.1897	0.0033	0.00014	0.00009
11	8/4	0.75	14.65	60.3	465	3281	115	4.9	1.8	0.2164	0.0076	0.00033	0.00012
12	8/4	0.75	8.03	60.3	467	3537	62	3.2	1.6	0.2333	0.0041	0.00021	0.00010
13	8/4	0.75	3.17	60.3	467	4000	73	3.4	2.1	0.2664	0.0048	0.00022	0.00014
14 ^a	8/4	1.0	8.62	60.3	467.5	3799	79	6.9	2.7	0.2518	0.0052	0.00046	0.00018

Notes are at the end of the table.

Table 1 (continued)

Run No.	Date	- Caustic Soda - gpm	At. Air P, psig ^b	EP Out T, °F	- B Conc., µg/m ³ - ave.	std. dev.	- Na Conc., µg/m ³ - ave.	std. dev.	- B Flow, lb/h --- ave.	std. dev.	- Na Flow, lb/h --- ave.	std. dev.
15	8/5	1.0	48.4	453	2701	99	2.2	2.0	0.1761	0.0065	0.00014	0.00013
16 ^a	8/5	1.0	60.3	455	2719	89	1.9	1.1	0.1779	0.0058	0.00013	0.00007
17	8/5	0.5	60.3	464	2915	69	2.4	1.1	0.1958	0.0046	0.00016	0.00008
18	8/5	0.52	60.3	474	2828	95	1.4	1.0	0.1887	0.0063	0.00009	0.00006
19	8/5	0.545	(60.3)	480	2326	68	0.9	1.1	0.1581	0.0046	0.00006	0.00008
20	8/5	0.5	60.1	484	6077	82	5.9	1.3	0.4101	0.0056	0.00040	0.00009
21	8/5	0.5	(60.1)	486	5702	164	6.0	4.1	0.3866	0.0112	0.00041	0.00028
22	8/5	0.75	(60.1)	487	6017	90	10.8	3.1	0.4123	0.0062	0.00074	0.00021
23	8/5	1.0	(60.1)	484	6649	76	7.5	3.3	0.4513	0.0051	0.00051	0.00022
24	8/5	1.25	(60.1)	480	6588	156	11.5	4.3	0.4498	0.0107	0.00078	0.00029
25 ^a	8/6	1.0	59.8	454	7265	58	0.014	0.028	0.4881	0.0039	9 x 10 ⁻⁷	19 x 10 ⁻⁷
26	8/6	1.0	80.9	455	6795	201	0	0	0.4589	0.0136	0	0
27	8/6	1.0	70.0	457	7023	131	4.8	2.6	0.4616	0.0086	0.00031	0.00017
28	8/6	1.0	48.9	458	7167	108	1.9	1.3	0.4747	0.0072	0.00013	0.00008

Notes are at the end of the table.

Table 1 (continued)

Run No.	Date	- Caustic Soda - lb Na/h	At. Air P, psig ^b	EP Out T, °F	- B Conc., µg/m ³ - ave.	std. dev.	- Na Conc., µg/m ³ - ave.	std. dev.	- B Flow, lb/h - - - ave.	std. dev.	- Na Flow, lb/h - - - ave.	std. dev.
29	8/6	0.5	70.0	468	7068	50	7.1	1.5	0.4797	0.0034	0.00048	0.00010
30	8/6	0.5	80.9	473	6059	122	3.3	2.3	0.4080	0.0082	0.00022	0.00015
31	8/6	0.5	59.3	478	5844	113	10.6	4.9	0.3926	0.0076	0.00071	0.00033
32	8/6	0.5	48.9	483	5606	69	8.4	4.2	0.3873	0.0048	0.00058	0.00029
33	8/6	1.25	48.9	482	5395	125	0.071	0.073	0.3758	0.0087	5 x 10 ⁻⁶	5 x 10 ⁻⁶
34	8/6	1.25	80.9	476	6418	155	1.6	1.5	0.4389	0.0106	0.00011	0.00011
35	8/6	1.25	70.0	468	6235	67	1.5	1.8	0.4095	0.0044	0.00010	0.00011
36	8/6	1.25	59.3	464	6687	117	5.5	2.7	0.4384	0.0077	0.00036	0.00018
37 ^a	8/6	1.0	59.3	464	6952	44	9.3	2.4	0.4727	0.0030	0.00063	0.00016

() Estimated by interpolation or extrapolation of other measurements.

a. Base case.

b. Corrected atomizing air pressure (last column of Table A2).

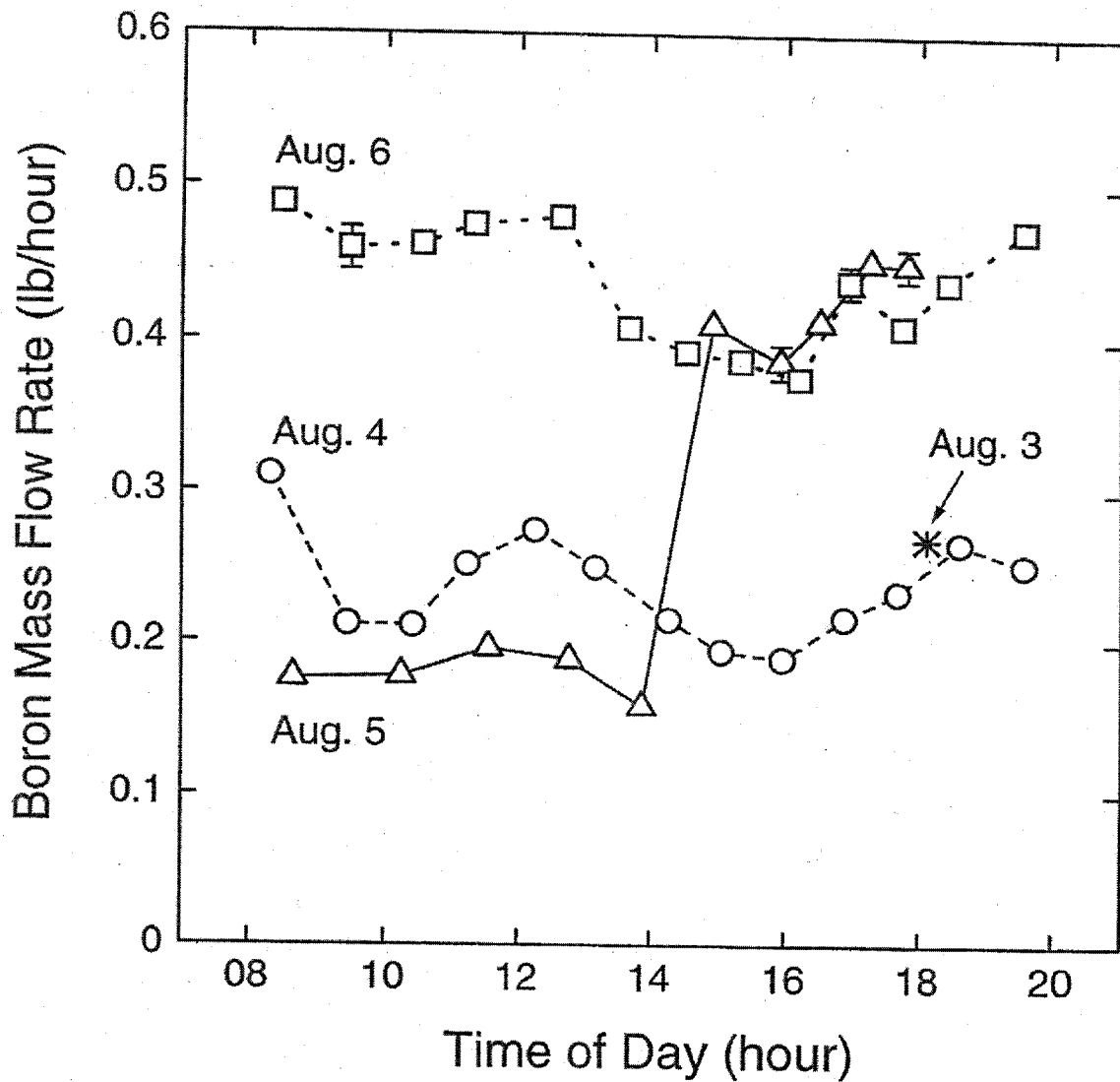


Figure 1. Mass flow rates of boron at the outlet from the electrostatic precipitator versus the time of day. The mass flow rates are the products of the concentration determined using laser-induced breakdown spectroscopy (LIBS) and the volumetric flow rate of flue gas determined from measurements of the gas velocity using a Pitot/static probe.

increase in boron concentration (Figure C3b), but the increase was followed by a decline in opacity that was not reflected in the boron measurements. A plot of boron concentration versus opacity, in Figure C4, shows that the boron measurements fall into two distinct groups, just as the data in Figure 1 clearly do, but that there is no significant correlation of the boron concentration with opacity. The absence of such a correlation may be explained by the fact that other streams are mixed with the flue gas before it enters the stack and the possibility that boron may still be largely in the form of vapor-phase species until the stack gas is cooled on mixing with ambient air in the plume. None of the other process data (Tables A1, A2, and A3) provide any evidence for a change in conditions that would explain why the boron measurements fall into two groups. Since we have no basis for discarding any of the data, all of it is retained for the analysis that follows, bearing in mind that, with the information available to us, changes in the actual boron concentration and the performance of the LIBS instrument are equally likely. The cause of the largest apparent change in boron concentration observed during the entire series of tests remains unknown.

Effect of Temperature

The correspondence between the minimum in boron flow rate and the maximum in ambient temperature suggests that temperature in the electrostatic precipitator has a significant influence on boron capture. The flow rate of boron is shown as a function of the temperature at the outlet from the precipitator in Figure 2. The high-boron group of data shows a systematic decrease in boron flow rate with increasing electrostatic precipitator outlet temperature, amounting to approximately a 15% decrease over the range of temperatures from 454 to 487 °F. Any such trend in the low-boron data is obscured by the changes that were being made in the sodium hydroxide feed to the caustic spray tower, discussed below.

The temperature in the horizontal flue between the vertical flue at the furnace exit and the caustic spray tower is very closely controlled (within about ± 2 °F, Figure A1, second panel from top) by adjustment of the quench water flow rate. The temperature at the outlet from the precipitator is determined by the caustic soda solution flow rate, the ambient temperature, and the intensity of solar radiation striking the ductwork, spray tower, and precipitator. The influence of the caustic soda flow rate, shown in Figure C5, indicates that the temperature at the inlet to the precipitator decreased by approximately 50 °F per gallon per minute of caustic soda solution. Much of the scatter in these data, roughly ± 10 °F is due to differences in the ambient temperature and its influence on the heat losses from the spray tower and ductwork. The temperature drop across the precipitator varied from 90 to 130 °F and was largely determined by the ambient temperature, as shown in Figure C6. A source of the scatter in these data is the variation in the position of the sun relative to the precipitator during the course of a day and the variation in intensity of solar radiation from day to day. The sum of the two temperature changes (quenching by caustic soda spray plus electrostatic precipitator), is approximately 160 °F (assuming a caustic soda flow rate of 1 gal/min), and accounts for somewhat less than half of the 355 °F drop in temperature between the entrance to the

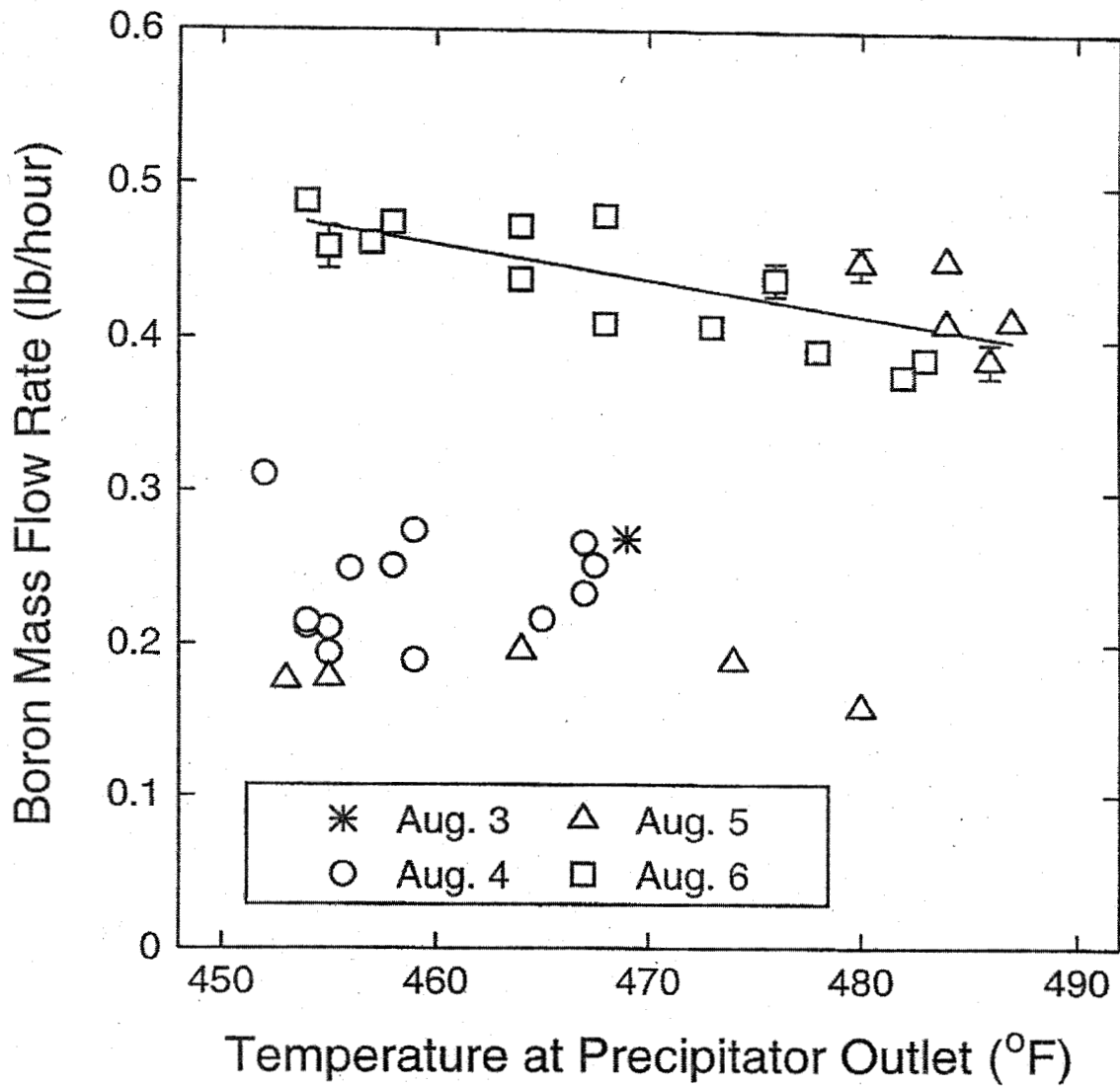


Figure 2. Mass flow rates of boron at the outlet from the electrostatic precipitator versus temperature at the outlet from the electrostatic precipitator.

horizontal flue and the outlet from the precipitator (825 to ~ 470 °F). The rest of the temperature drop is due to the convective losses from the flues and spray chamber.

Effect of Sodium Feed Rate

Because the sensitivity of the boron flow rate at the outlet from the electrostatic precipitator to the outlet temperature is not too great (Figure 2), the effects of other process conditions can be examined in the absence of a significant influence of temperature by dividing the data into two groups: (1) those having precipitator outlet temperatures in the range from 452 to 469 °F and (2) those having precipitator outlet temperatures in the range from 473 to 487 °F. The dependence of the boron flow rates in the flue on the sodium feed rate (pounds of the element Na per hour) to the caustic spray tower for the high and low ranges of precipitator outlet temperature are shown in Figures 3a and 3b, respectively.

The measurements at low precipitator outlet temperature on August 3, 4, and 5 (Figure 3b: asterisk, circle, and triangle symbols, respectively) show a slight but systematic decrease with increasing sodium feed. A similar trend is shown by the high-boron group of data at high precipitator outlet temperature (Figure 3a: square and triangle symbols at upper left). The slopes of the two lines drawn through the points in Figure 3 for high and low precipitator outlet temperatures are - 0.00345 and - 0.00372 lb boron/lb sodium, respectively, for an average value of 0.00359 pounds of boron removed from the flue per pound of sodium fed to the spray tower. Dividing by the ratio of the atomic weights of boron and sodium ($10.81/22.99 = 0.47$) to convert to a molar basis, we find that the apparent incremental effect of sodium on the removal of boron is only 0.0076 atom of boron per atom of sodium injected into the caustic spray tower. It is perhaps significant that no high boron flow rates were observed when the sodium feed rate was above about 8.5 lb/h.

Effect of Caustic Soda Atomizing Air Pressure

Increasing the pressure of air supplied to the caustic soda spray nozzle, with other conditions fixed, increases the mass flow rate of the atomizing air and the ratio of the air to liquid flow rates, which shifts the droplet size distribution to smaller sizes. This increases the surface area per unit mass of the sodium hydroxide residues left when the droplets dry out, which would be expected to increase the effectiveness of the sodium hydroxide for boron and sulfur capture. On the other hand, smaller droplets are decelerated more rapidly as the spray mixes with surrounding gas, so a shift to smaller droplet sizes may have the disadvantage that the spray is less well mixed with the flue gas stream. A good discussion of sprays and the effects of atomizing conditions on mean droplet size may be found in the book by Lefebvre (1989).

The results from the experiments in which the atomizing air pressure was varied are shown in Figures 4a and 4b, divided into two groups according to the precipitator outlet temperature, as in Figures 3a and 3b. The symbols in Figure 4 represent different caustic soda flow rates, not different days of testing, as they did in previous figures.

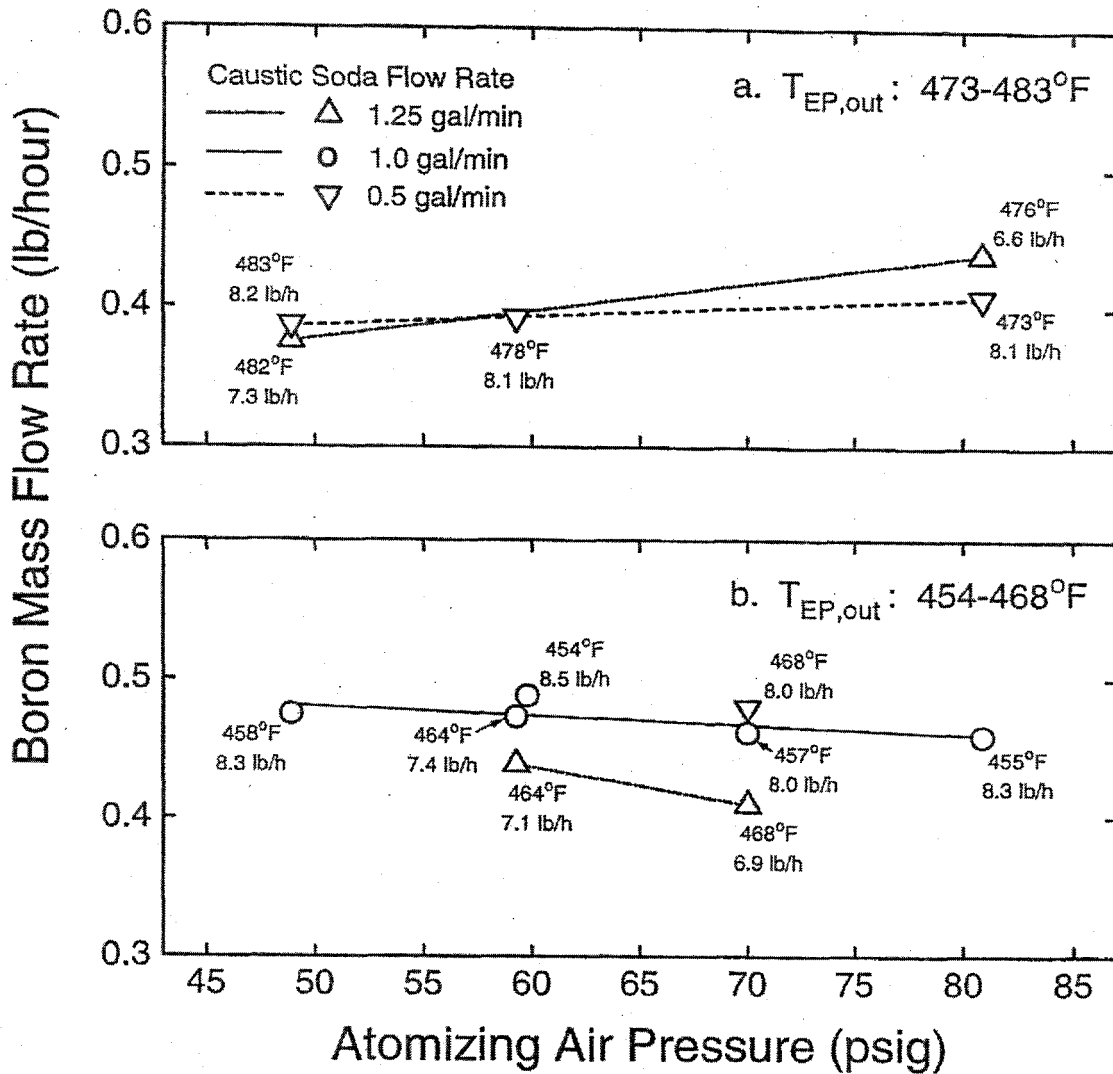


Figure 4. Mass flow rates of boron at the outlet from the electrostatic precipitator versus the pressure of the caustic soda atomizing air.

- Electrostatic precipitator outlet temperatures in the range from 473 to 483 °F.
- Electrostatic precipitator outlet temperatures in the range from 454 to 468 °F.

The numbers next to the data points give the temperature at the electrostatic precipitator outlet and the sodium feed rate to the caustic soda spray tower during each run. The triangle, circle, and inverted triangle symbols here indicate different caustic soda flow rates rather than different days of testing, as they did in Figures 1-3.

Sodium feed rates to the spray tower during the measurements were in the range from 6.6 to 8.5 lb/h. Because the effect of the atomizing air pressure is evidently weak, the precipitator outlet temperature and sodium feed rate are specified next to each data point, so that the effects of these conditions may be taken into consideration when examining the trends. All of the data are from the high-boron group of measurements, in the vicinity of 0.4 to 0.5 lb boron/h.

A slight decrease in boron flow rate with increasing air pressure is shown by the measurements at 1.0 gal/min caustic soda flow rate (Figure 4b: circles), but the effect is small. The two points in Figure 4b at the caustic soda flow rate of 1.25 gal/min are not enough to establish a trend. Just the opposite behavior is shown by the data in Figure 4a, but the effect of the air pressure is again very weak, especially for the more reliable of the two data sets, at the caustic soda flow rate of 0.5 gal/min, for which there are three data points (inverted triangles). However, for these three measurements there is a systematic decrease in the precipitator outlet temperature with increasing atomizing air pressure, which may have masked or offset the effect of the pressure alone. The 10 °F decrease in temperature would cause an increase of approximately 0.02 lb/h in the boron flow rate, according to the line drawn through the high-boron points in Figure 2. Accounting for this effect would decrease the slope of the line for the 0.5 gal/min case in Figure 4a. We conclude that the dependence of boron capture on the caustic soda atomizing air pressure is the weakest of the effects investigated and that even the direction of the effect cannot be reliably determined from the data. The practical implication is that the atomizer might as well be run at pressures toward the low end of the manufacturer's recommended range since increasing pressure increases gas and liquid velocities and the rate of atomizer wear. The condition of the atomizer tip has a strong influence on spray quality.

Comparison with the Boron Measurements in August 2000

The oxygen to natural gas ratio during the present tests was 1.86, close to the base case value of 1.85 during the tests in August 2000. The boron flow rate at the outlet from the electrostatic precipitator during the August 2000 tests, under the base test condition, was reported as 0.065 ± 0.003 lb/h. However, the flue gas volumetric flow rate determined by the traverses of the duct in August 2001 is a factor of 1.7 greater than the estimate used to calculate the mass flow rates a year earlier. Making this correction increases the boron flow rate in August 2000 to 0.11 ± 0.01 lb/h. The base case run condition of August 2001 was repeated six times over the course of the tests (runs 1, 2, 14, 16, 25, and 37) with an average boron flow rate of 0.33 ± 0.13 lb/h, a significant increase over the boron flow rate under the base condition of a year earlier, when the indicated density of the caustic soda solution was 1.09, compared to densities in the range from 1.040 to 1.045 under the base condition during the present tests.

During the measurements downstream from the electrostatic precipitator in August 2000, the sodium feed rate to the caustic spray tower was 22.9 lb/h, assuming the calibration of the density meter did not change during the year between the tests, and the temperature at the outlet from the precipitator was in the range from 444 to 459 °F. Referring to Figure 3b in the present report, whose temperatures overlap this range, and

using the equation for the line shown in the figure (Boron flow rate in lb/h = $0.268 - 0.00372 \times$ Sodium feed rate in lb/h) we find a boron flow rate of 0.18 lb/h, compared with the flow rate of 0.11 lb/h a year ago.

The effect of electrostatic precipitator temperature on boron capture (Figure 2) raises the question whether changes in temperature might have influenced the apparent dependence of the boron flow rate at the outlet from the precipitator on the oxygen to gas ratio in the furnace observed in August 2000 and presented in Figure 10 of the report by Walsh, Johnsen, and Ottesen (2001, p. 23). The data answering this question are attached as Appendix G. The boron flow rates from August 2000 are shown as a function of the time of day in Figure G1a along with the oxygen to gas ratios, shown in Figure G1b. The behavior of the boron flow rate through the day, which peaks shortly after 16:00 hours, is quite different from the pattern shown by the data in Figure 1, in which there is a minimum near that time. Comparison of Figure G1a with Figure G1b shows that the pattern of the boron flow rates primarily reflects the pattern of the oxygen-to-gas ratios, as concluded in the report of the August 2000 test. A plot of the boron flow rates versus the temperature at the outlet from the electrostatic precipitator, shown in Figure G2, confirms that there was no systematic effect of the precipitator outlet temperature on the results. It is still possible that an effect of temperature is embedded in the data but obscured by the effects of the changes in oxygen-to-gas ratio.

Sodium

Time Dependence

The variation of sodium flow rate at the precipitator outlet with time of day during all of the tests is shown in Figure 5, suggesting a tendency for sodium in the flue to increase as the day progresses, a different behavior from that of boron (Figure 1). The mode of occurrence of sodium is also quite different from that of boron. Whereas boron is typically observed in 50% or more of the laser sparks, indicating that it is uniformly distributed as vapor or fine particles, sodium is observed only rarely but at high concentration, indicating that it is present as large particles or agglomerates at low number concentration. The mechanism of penetration of sodium through the precipitator is evidently by re-entrainment. Since the mechanisms by which boron and sodium pass through the precipitator are entirely different, there is no correlation between the boron and sodium flow rates. The sodium data also do not fall into two distinct groups, as the boron measurements did.

The most significant feature of the sodium measurements is that the average flow rates are extremely low. The low frequency with which sodium is observed and its low average concentration account for the large values of the standard deviation of the 1000-shot averages, indicated by the error bars in Figure 5. When sodium was observed in a laser spark, it was not uncommon for its concentration and the emission intensity to be so high that the detector was saturated. This would cause the intensity, and therefore the sodium concentration, to be underestimated, so the actual average sodium flow rates may

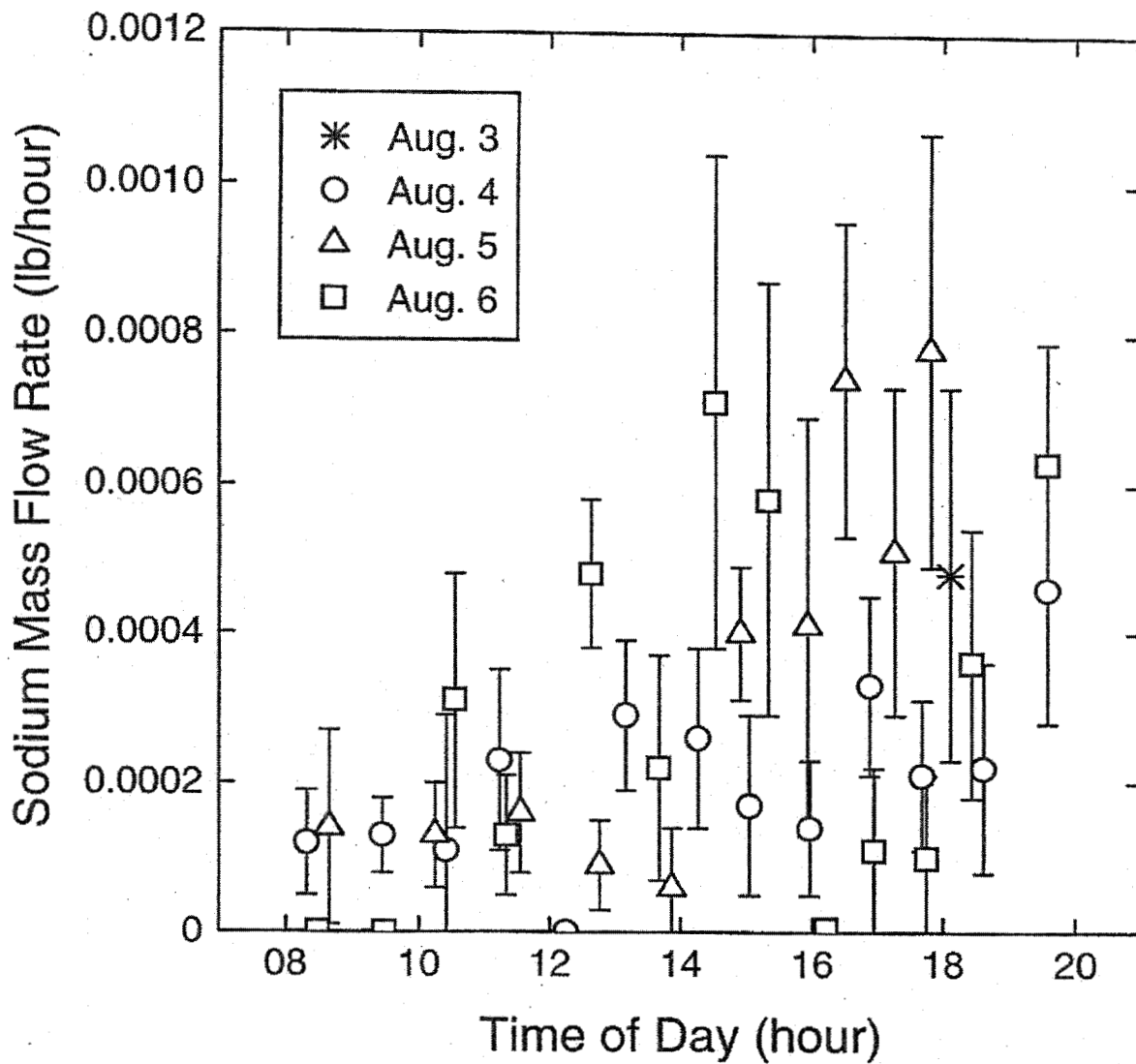


Figure 5. Mass flow rates of sodium at the outlet from the electrostatic precipitator versus the time of day. The length of the error bars is one standard deviation of the results from multiple (usually six) 1000-shot average LIBS spectra.

be somewhat higher than the reported values (Table 1 and Figures 5-8), but probably not by more than a factor of two.

Effect of Temperature

The dependence of the sodium flow rates on temperature at the electrostatic precipitator outlet is shown in Figure 6. While the data may suggest an increase in sodium flow rate with increasing temperature, the large random fluctuations in sodium concentration make it impossible to establish a trend with any certainty.

Effect of Sodium Feed Rate

The dependence of the flow rate of sodium at the outlet from the precipitator on the feed rate of sodium to the caustic spray tower is shown in Figure 7. The data are divided into two groups according to the temperature at the outlet from the precipitator, as was done for boron in Figure 3. The sodium leaving the precipitator has no discernable systematic dependence on its feed rate. This is consistent with its source being re-entrainment, in which case its penetration would not depend so much on the amount of sodium collected as on other factors such as the rapping frequency.

Effect of Caustic Soda Atomizing Air Pressure

Not surprisingly, in view of the results for boron and sodium already considered, no systematic dependence of the sodium flow rate at the precipitator outlet on the caustic soda atomizing air pressure is visible in the data, shown in Figure 8.

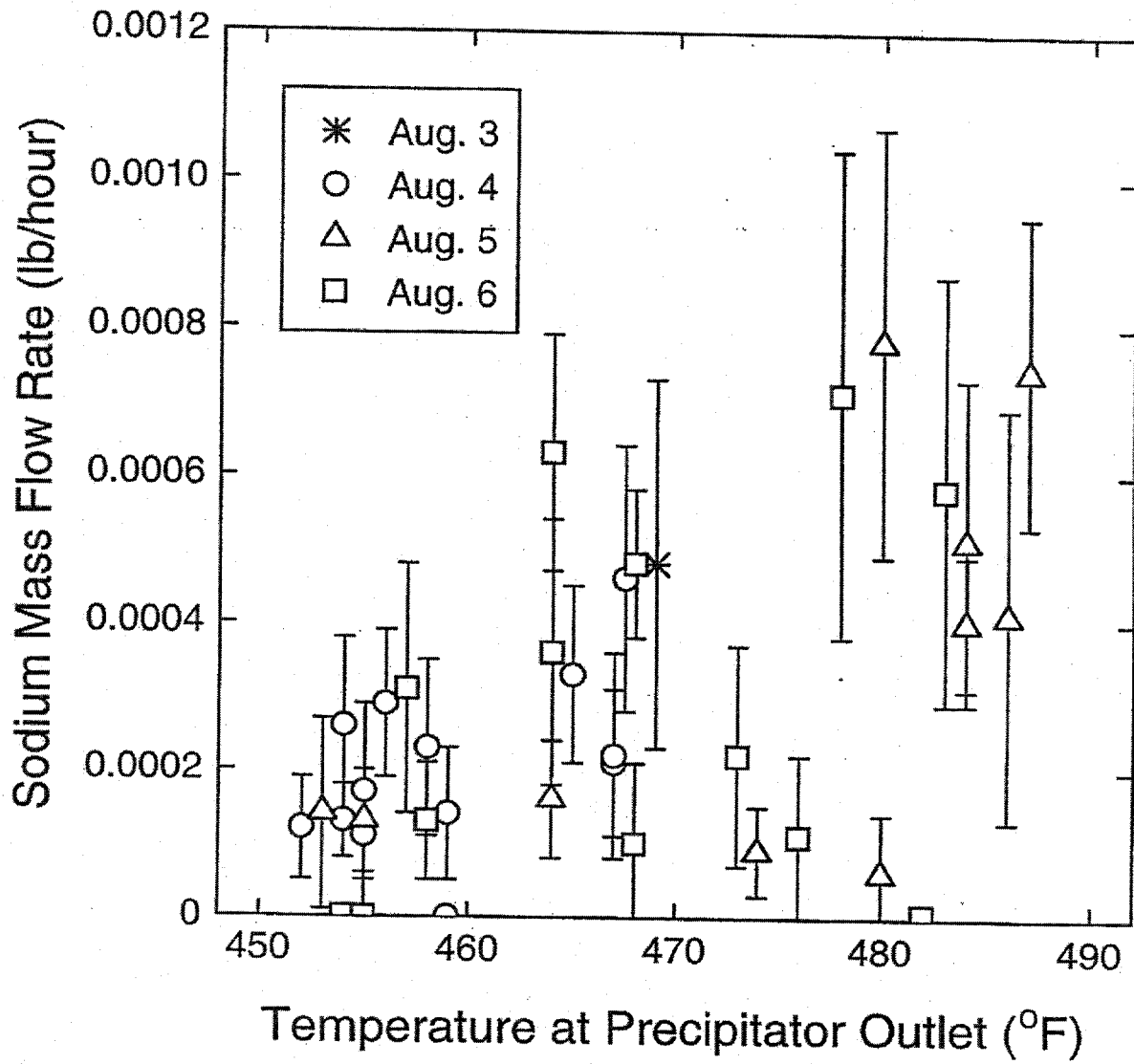


Figure 6. Mass flow rates of sodium at the outlet from the electrostatic precipitator versus temperature at the outlet from the electrostatic precipitator.

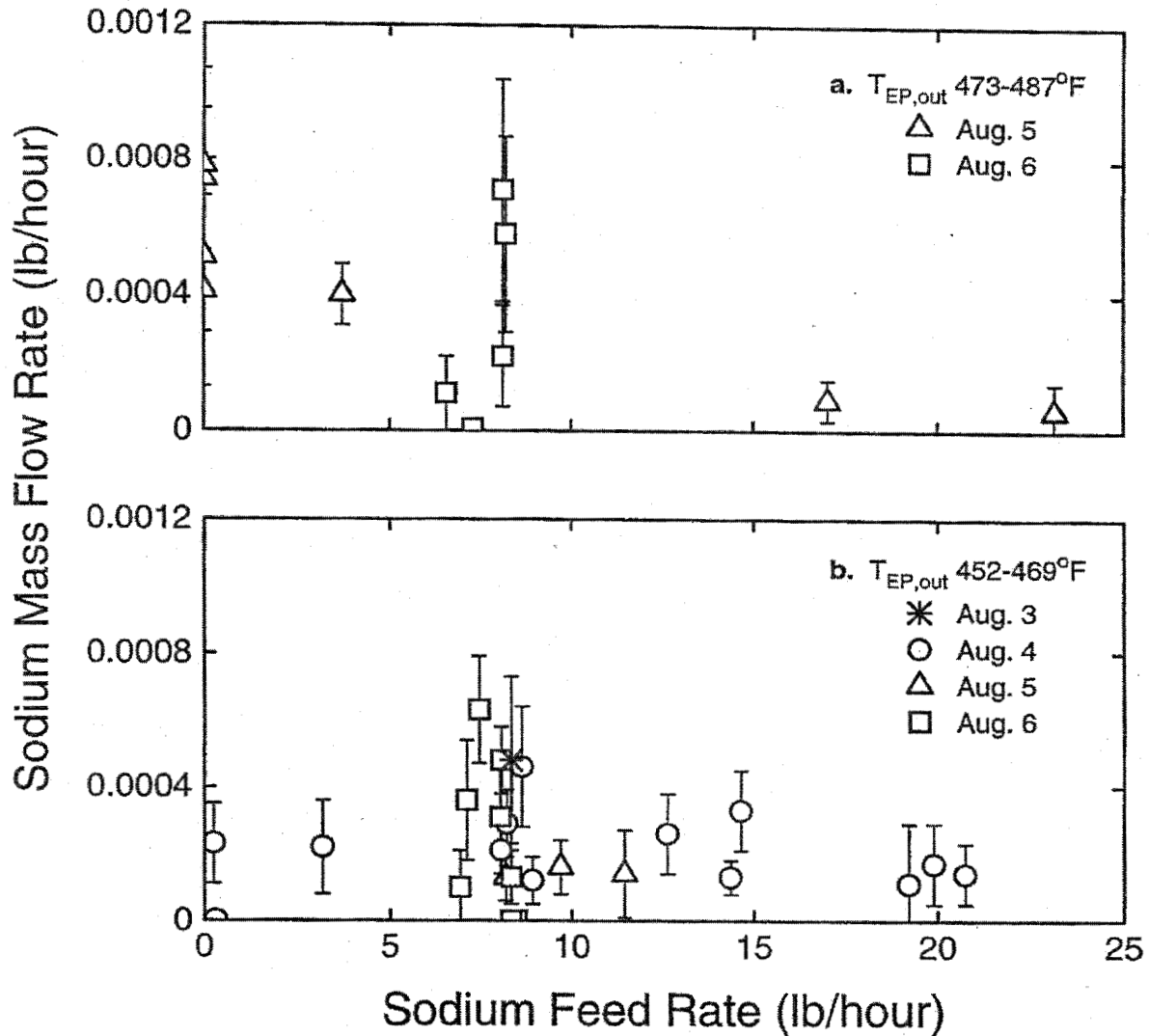


Figure 7. Mass flow rates of sodium at the outlet from the electrostatic precipitator versus the feed rate of sodium (as the element, Na) to the caustic soda spray tower.

- Electrostatic precipitator outlet temperatures in the range from 473 to 487 °F.
- Electrostatic precipitator outlet temperatures in the range from 452 to 469 °F.

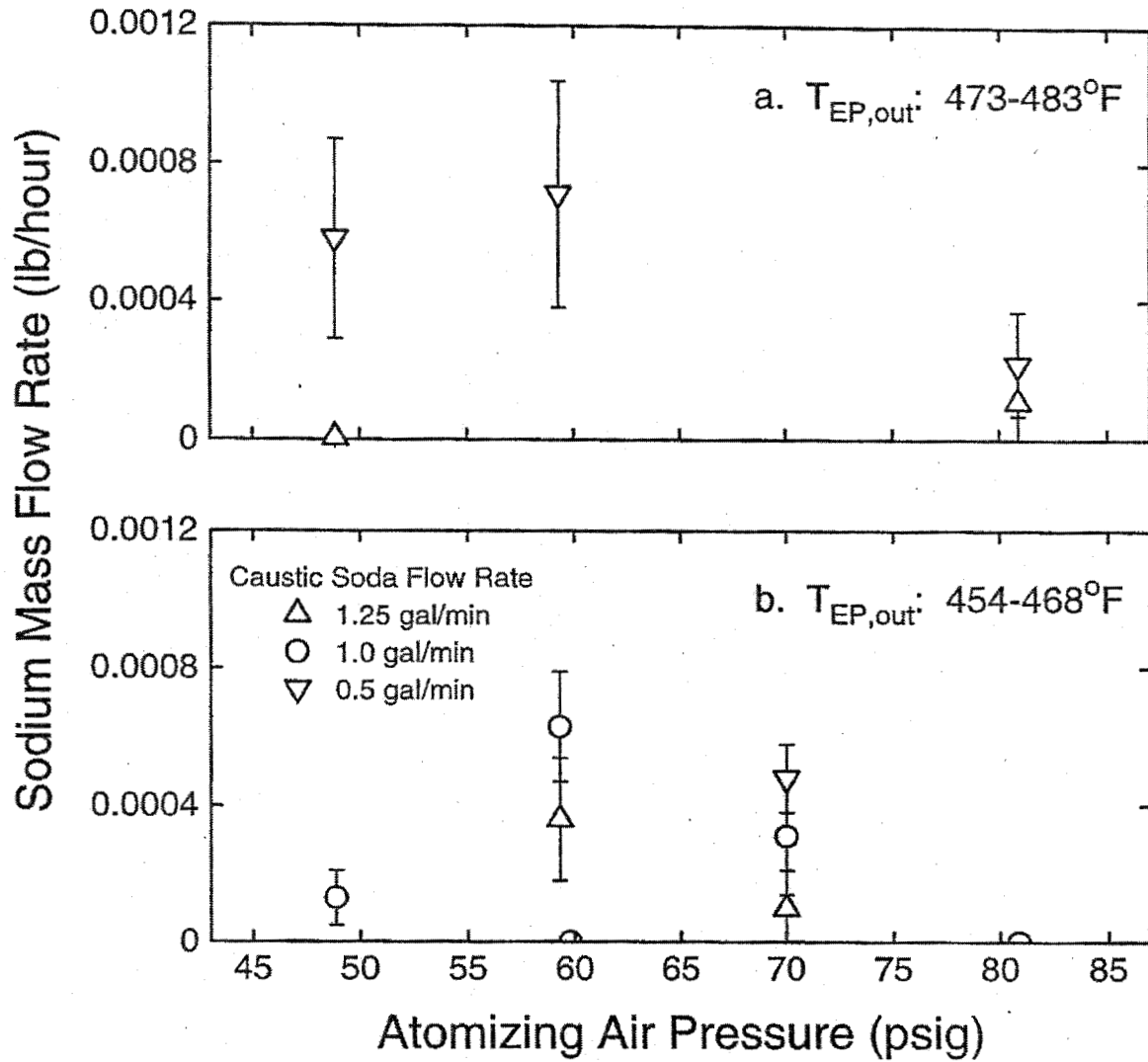


Figure 8. Mass flow rates of sodium at the outlet from the electrostatic precipitator versus the pressure of the caustic soda atomizing air.

- a. Electrostatic precipitator outlet temperatures in the range from 473 to 483 °F.
- b. Electrostatic precipitator outlet temperatures in the range from 454 to 468 °F.

EQUILIBRIUM MODEL CALCULATIONS

Interpretation of the experimental results is facilitated by comparison with the temperature and sodium concentration dependences of solid particle composition and vapor species concentrations predicted at full chemical equilibrium under the conditions in the electrostatic precipitator. In the presence of the continuous decrease in temperature of the gas and particles as they pass through the precipitator, the system could not be said to be at true equilibrium, but the residence time in the precipitator may be long enough, and the rate of change in temperature slow enough, for the system to approach its local equilibrium composition. The NASA Chemical Equilibrium with Applications (CEA) Code (Gordon and McBride, 1994; McBride and Gordon, 1996) was used to determine the equilibrium composition.

The mole fractions of the major gaseous components of the flue gas were calculated using the same code (Appendix E) used to determine the average molecular weight of the gas in the calculation of its flow rate, taking into consideration the gas and oxygen feeds, gas composition, oxygen composition, batch gases, the oil used to wet the batch, inleakage of air, the humidity of the air, quench water, and water introduced into the caustic spray tower. The concentrations of boron, sulfur, and potassium were calculated from an estimate of the typical rate of dust collection in the electrostatic precipitator under the base case conditions (115 lb/h, including 11.62 lb/h of Na_2O formed from the caustic soda) and the composition of the dust sample (Appendix F). The concentration of Na was varied to examine its effects. The elements considered in the equilibrium calculations were Na, K, B, S, H, O, C, and N.

According to the NASA CEA Code and its database of thermodynamic properties, the following Na, K, B, and S species are the only ones present at significant concentrations under the conditions of composition, pressure, and temperature in the electrostatic precipitator: Na_2SO_4 , K_2SO_4 , Na_2CO_3 , NaBO_2 , $\text{Na}_2\text{B}_4\text{O}_7$, and H_3BO_3 . $\text{H}_3\text{B}_3\text{O}_6$ is also present, but only at concentrations negligible with respect to those of H_3BO_3 , under the conditions examined. Sodium tetraborate, $\text{Na}_2\text{B}_4\text{O}_7$, whose presence in the dust was predicted by Beerkens and van Limpt (2001), was not included in the NASA CEA thermodynamic database when the calculations were first undertaken. Discrepancies between the initial calculations and the experimental results suggested that $\text{Na}_2\text{B}_4\text{O}_7$ was an important component of the dust. Bonnie J. McBride, of the NASA Glenn Research Center, responded very quickly to our request for thermodynamic data for sodium tetraborate, so it could be added to the database for the calculations described below.

Under the assumption that all the major species stable under the conditions of interest were included in the NASA CEA Code's thermodynamic database, the fate of

volatilized sodium and potassium, sulfur dioxide from batch decomposition and fining, and sodium hydroxide added at the spray tower can be generally summarized as follows:

1. All of the potassium appears in the precipitator dust as solid potassium sulfate, K_2SO_4 ,
2. The remaining sulfur dioxide forms solid sodium sulfate, Na_2SO_4 ,
3. The remaining sodium first forms solid sodium tetraborate, $Na_2B_4O_7$,
4. If there is not enough sodium to react with the boron, the excess boron forms orthoboric acid, H_3BO_3 , plus a small amount of the metaboric acid trimer, $H_3B_3O_6$, which are gases at the temperatures in the precipitator,
5. If there is more sodium than needed to react with the boron, the excess forms solid sodium carbonate, Na_2CO_3 , below about 490 °F,
6. Above 490 °F, excess sodium forms sodium metaborate, $NaBO_2$, at the expense of sodium tetraborate, and
7. Even when there is a large excess of sodium, the reaction of sodium with orthoboric acid is not complete, allowing a small concentration of H_3BO_3 to remain in the vapor phase. This relatively small amount of vapor is the source of the difficulty in removing the last traces of boron from the flue gas.

According to this picture, the chemical system in the electrostatic precipitator can be described as having two regimes, depending upon whether the total of the sodium and potassium concentrations is greater or less than the concentration required for stoichiometric reaction with boron and sulfur species to form K_2SO_4 , Na_2SO_4 , and $Na_2B_4O_7$. The parameter distinguishing the two regimes is the molar ratio, $(Na+K)/(\frac{1}{2}B+2S)$, which can be evaluated by analysis of the precipitator dust, assuming that the fraction of any of these elements not captured in the precipitator is small. The ratio can also be expressed in terms of the relative numbers of moles of the oxides of the elements in the dust, $(Na_2O+K_2O)/(\frac{1}{2}B_2O_3+SO_3)$, if this is more convenient. We refer to this quantity as the "alkali to boron-plus-sulfur ratio," and proceed to an examination of the equilibrium composition of the system in the precipitator as a function of this parameter and temperature. The alkali to boron-plus-sulfur ratio will be changed by varying the sodium concentration, keeping the potassium, boron, and sulfur concentrations fixed at values corresponding to the dust analysis given in Appendix F. A system having an alkali to boron-plus-sulfur ratio smaller than 1 contains less sodium than needed to convert all of the boron to sodium tetraborate and vice versa.

From the analysis of the dust sample taken from the electrostatic precipitator under the base run condition (Appendix F), we find the following numbers of moles of individual elements in 100 g of dust: K, 0.1187; Na, 0.9610; S, 0.2817; C, 0.0883; B, 0.8475; Ca, 0.0137; and Mg, 0.0079. The alkali to boron-plus-sulfur ratio in the dust is then 1.094. (One might want to refine this argument a bit by accounting for the capture of some sulfur as calcium and magnesium sulfates. This could be done by subtracting the numbers of moles of calcium and magnesium from sulfur. The alkali to boron-plus-sulfur ratio would then be $[Na+K]/[\frac{1}{2}B+2(S-Ca-Mg)]$. For the dust analysis given above the value of this ratio is 1.144.) We consider the results of equilibrium calculations for four cases, starting at a low alkali to boron-plus-sulfur ratio and progressively increasing the sodium concentration to the level corresponding to the observed composition of the dust sample. We use the simpler, approximate, definition of the alkali to boron-plus-sulfur ratio, $(Na+K)/(\frac{1}{2}B+2S)$.

The first case is one in which the sodium concentration is significantly smaller than the amount required to maximize capture of boron by sodium, i.e. $(\text{Na}+\text{K})/(\frac{1}{2}\text{B}+2\text{S}) = 0.96$. Mole fractions of the most abundant stable species under this condition are shown as a function of temperature in Figure 9. The range of temperatures was chosen to span the entire range likely to have been present in the electrostatic precipitator during the tests, from the lowest outlet temperature, 452 °F, to the highest inlet temperature, 605 °F. The mole fractions are those for the entire gas/particle mixture, assuming that the solid species remain suspended, i.e. the number of moles of each component per mole of gas (H_2O , CO_2 , O_2 , N_2 , etc.) plus solid species.

As shown in Figure 9, there is no significant dependence of the K_2SO_4 , Na_2SO_4 , $\text{Na}_2\text{B}_4\text{O}_7$, or H_3BO_3 mole fractions on temperature when the sodium concentration is much lower than the amount required for complete reaction with boron. Because there is too little sodium, a rather large concentration of orthoboric acid, H_3BO_3 , remains unreacted in the vapor phase and would be expected to pass through the precipitator. Its concentration, 58 mol ppm, corresponds to a flow rate of 1.0 lb/h of boron (as the element, B) leaving the precipitator, more than twice the highest measured flow rates (Figure 1).

The results for a case in which sodium is closer to, but still slightly below, the stoichiometric amount, $(\text{Na}+\text{K})/(\frac{1}{2}\text{B}+2\text{S}) = 0.98$, are shown in Figure 10. Compared with the previous case, the additional sodium has converted more H_3BO_3 to the sodium borates, $\text{Na}_2\text{B}_4\text{O}_7(\text{solid})$ and $\text{NaBO}_2(\text{solid})$. On the left in Figure 10, below about 510 °F, the remaining orthoboric acid vapor is now 29 mol ppm, corresponding to a boron flow rate of 0.5 lb/h leaving the precipitator, near the upper limit of the measured flow rates (Figure 1). Above 510 °F, the concentration of H_3BO_3 increases with increasing temperature, coinciding with the appearance of NaBO_2 , whose concentration increases exactly in parallel with that of H_3BO_3 . The total of the increases in H_3BO_3 and NaBO_2 corresponds exactly, mole for mole, to the decrease in $\text{Na}_2\text{B}_4\text{O}_7$ with increasing temperature (times 4, since there are 4 boron atoms in each $\text{Na}_2\text{B}_4\text{O}_7$). There is no change in either K_2SO_4 or Na_2SO_4 with temperature and no change from their values in Figure 9. Assuming that the NASA CEA database contains all of the sulfur compounds that are stable under these conditions, there is evidently no other place where sulfur would like to go (the small amounts of CaO , MgO , and other species in the precipitator dust that might react with SO_2 were not included in the calculation).

The result of another increase in sodium, to the stoichiometric amount for conversion of sulfur and boron to K_2SO_4 , Na_2SO_4 , and $\text{Na}_2\text{B}_4\text{O}_7$, $(\text{Na}+\text{K})/(\frac{1}{2}\text{B}+2\text{S}) = 1.00$, is shown in Figure 11. In spite of the increase in sodium, there are only slight decreases in the H_3BO_3 mole fractions compared to the previous case, in the temperature range below 510 °F. Above 510 °F, the H_3BO_3 concentrations are identical to those in Figure 10. The sodium not reacting with boron is seen to be present as Na_2CO_3 below about 490 °F and as NaBO_2 at higher temperatures. The concentrations of H_3BO_3 vapor are now at the lowest levels that can be achieved by addition of sodium to the system, over the entire range of temperatures shown. The temperature dependence of H_3BO_3 is

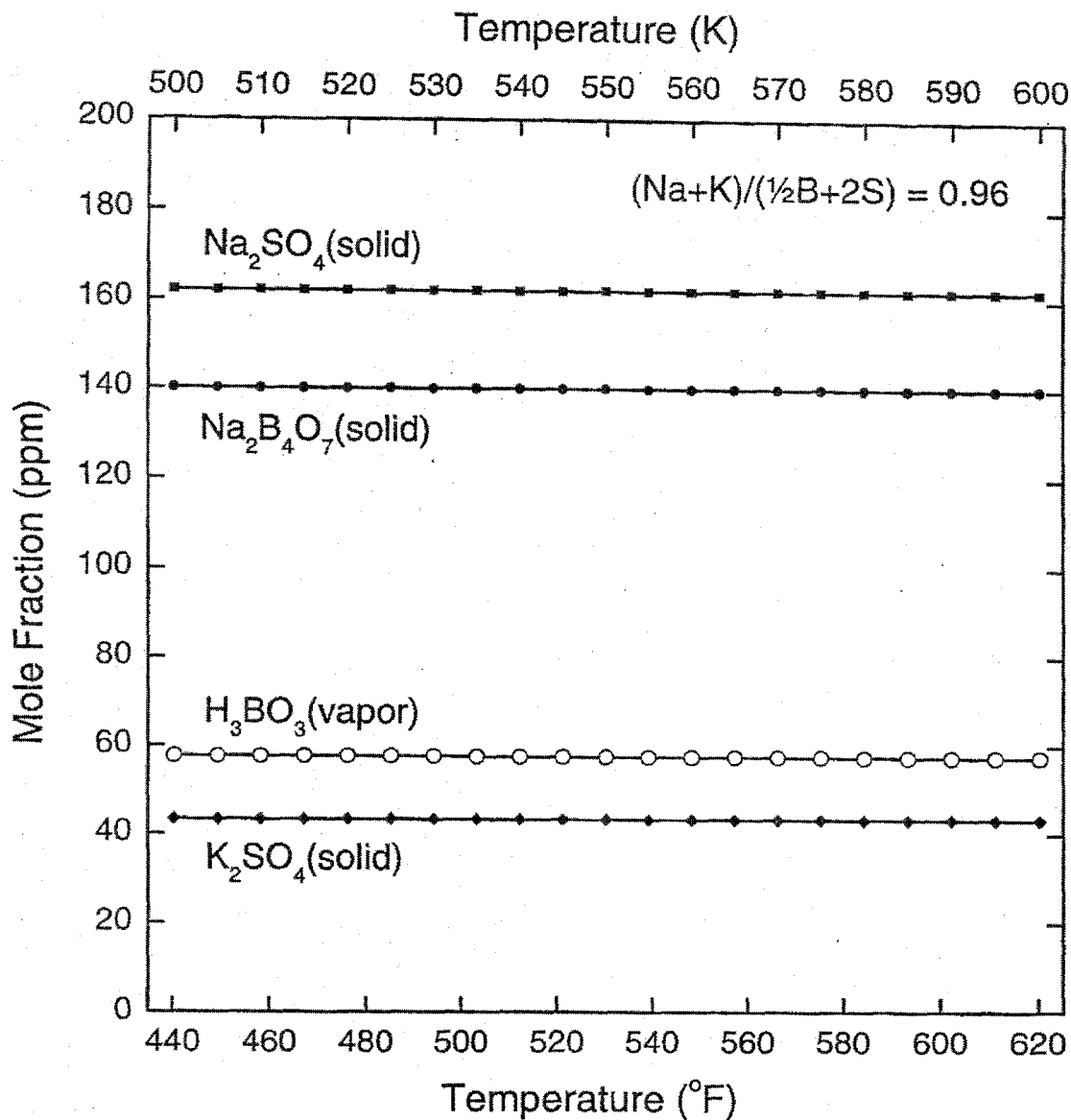


Figure 9. Results of calculations using the NASA Chemical Equilibrium with Applications (CEA) Code and thermodynamic property database (Gordon and McBride, 1994; McBride and Gordon, 1996; McBride, 2002) showing the predicted mole fractions of boron, sodium, potassium, and sulfur species at full chemical equilibrium in the range of temperatures present in the electrostatic precipitator during the tests (lowest outlet to highest inlet temperature) and with an alkali to boron-plus-sulfur mole ratio of 0.96. The relative amounts of boron, potassium, and sulfur in the system were chosen to reflect the dust sample composition (Appendix F) and the sodium was adjusted to give the specified alkali to boron-plus-sulfur ratio.

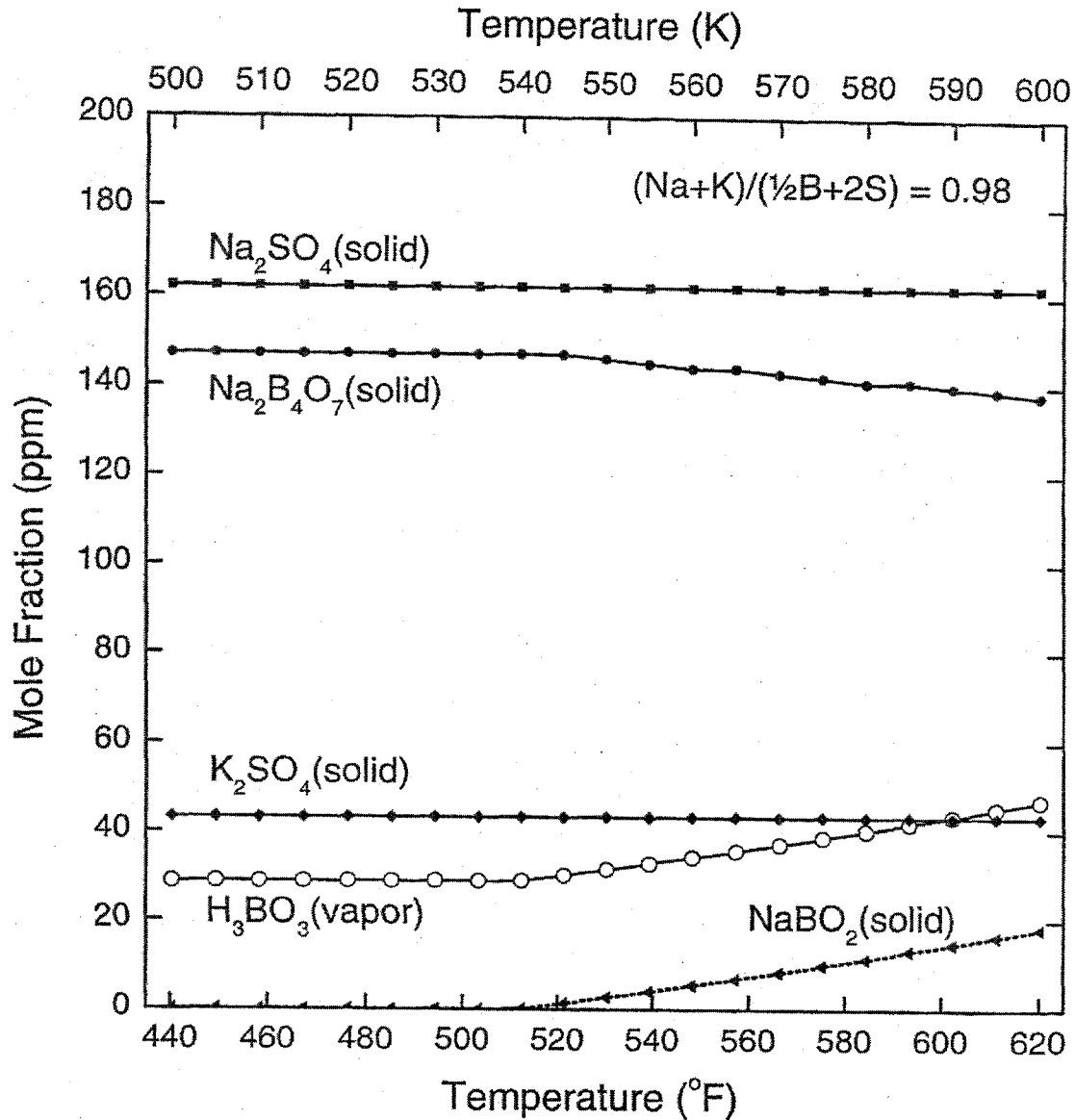


Figure 10. Results of calculations of equilibrium chemical composition in the electrostatic precipitator, similar to those shown in Figure 9, but with the sodium increased to give an alkali to boron-plus-sulfur ratio of 0.98. As a result of the increased sodium content, the mole fractions of $\text{Na}_2\text{B}_4\text{O}_7$ are higher, and the H_3BO_3 vapor mole fractions lower than in Figure 9. In this case, excess sodium over the amount needed to reduce the H_3BO_3 mole fraction to its lowest possible level forms NaBO_2 at temperatures above about 510 °F.

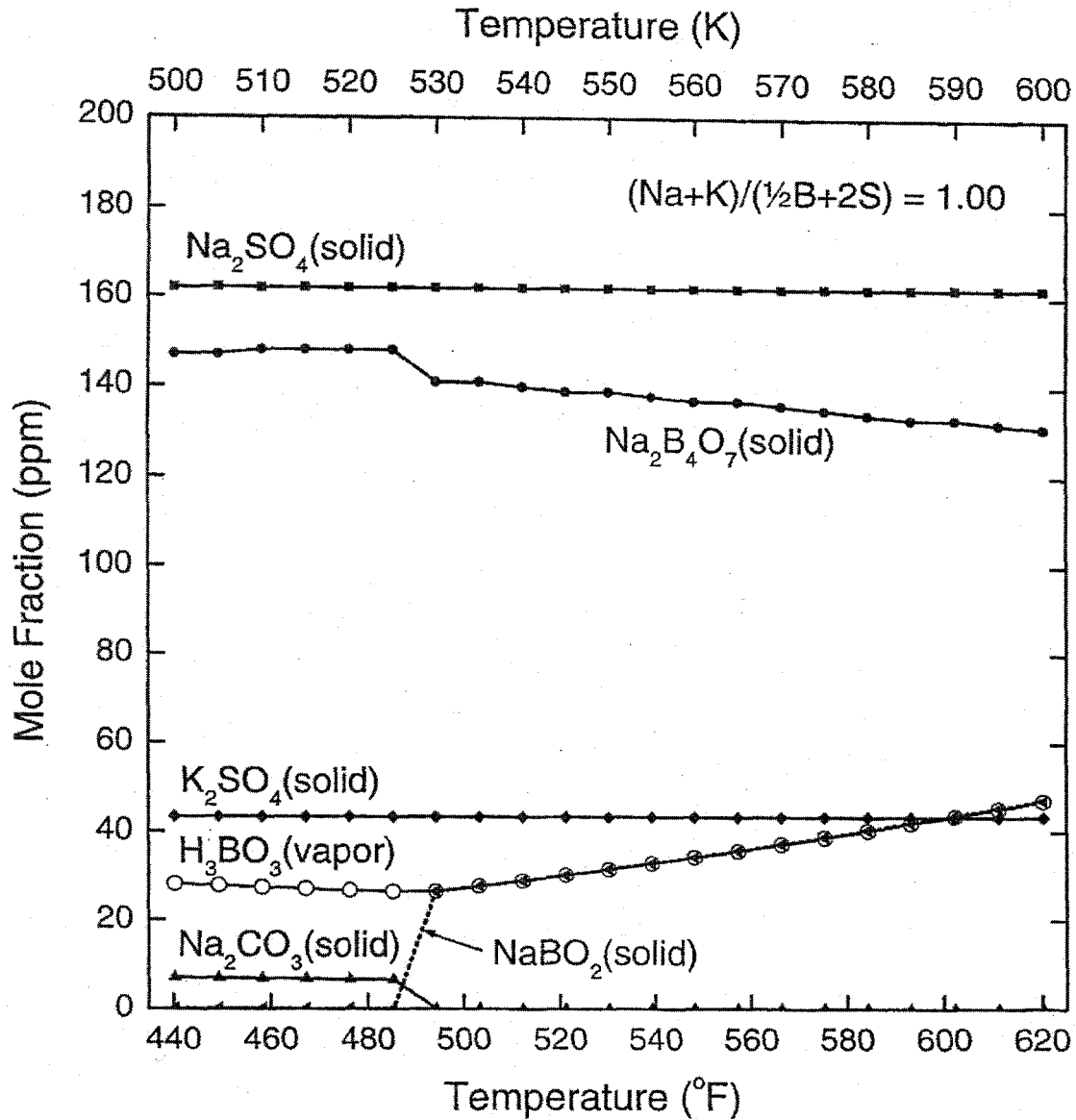
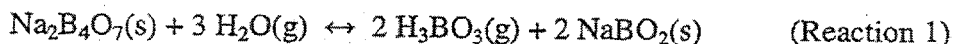


Figure 11. Results of calculations of equilibrium chemical composition in the electrostatic precipitator, similar to those shown in Figures 9 and 10, but with the sodium increased to give an alkali to boron-plus-sulfur ratio of 1.00. The sodium content of the system is now in excess of the amount sufficient to reduce H₃BO₃ to its minimum possible level over the whole range of temperatures shown. Excess sodium forms sodium carbonate at temperatures below about 490 °F and reacts with sodium tetraborate to form sodium metaborate at temperatures above 490 °F.

interesting, its concentration decreasing with increasing temperature from 440 to 490 °F, then increasing with temperature above 490 °F. We will return to this observation again later, in the Discussion Section. In this stoichiometric case, the mole fractions of H_3BO_3 and NaBO_2 are equal when NaBO_2 is present and Na_2CO_3 is absent, above about 495 °F (sideways triangles and open circles superimposed on the right in Figure 11), reflecting their relationship through the reaction



There is no change in either K_2SO_4 or Na_2SO_4 from their fixed mole fractions of the previous two examples.

As shown above, the alkali to boron-plus-sulfur ratio in the dust sample from the electrostatic precipitator at the base case test condition (Appendix F) was $(\text{Na}+\text{K})/(\frac{1}{2}\text{B}+2\text{S}) = 1.094$. The result of increasing the sodium concentration to this level is shown in Figure 12. Below about 485 °F, all of the additional sodium above that in the previous case reacts with CO_2 to form Na_2CO_3 . Above about 495 °F, the additional sodium reacts with $\text{Na}_2\text{B}_4\text{O}_7$ to form NaBO_2 , as in Figure 11. However, both the sodium carbonate and sodium metaborate concentrations are now much higher, due to the relatively large excess of sodium. There is no change in the H_3BO_3 vapor mole fractions, compared with the case shown in Figure 11. Therefore, above the level of sodium needed for complete capture of sulfur and reaction with boron to form $\text{Na}_2\text{B}_4\text{O}_7$, there appears to be no benefit, from the point of view of suppressing H_3BO_3 vapor, to be gained from further sodium addition.

The H_3BO_3 vapor concentrations from Figures 9 and 10 are shown on an expanded scale in Figure 13, along with calculations for other alkali to boron-plus-sulfur ratios, $(\text{Na}+\text{K})/(\frac{1}{2}\text{B}+2\text{S}) = 0.95, 0.97, \text{ and } 0.99$. The curve shown for the mole ratio of 0.99 is identical to those for the ratios of 1.00 in Figure 11 and 1.094 in Figure 12, because the sodium added to take the system from $(\text{Na}+\text{K})/(\frac{1}{2}\text{B}+2\text{S}) = 0.99$ to 1.00 and 1.094 forms sodium carbonate or sodium metaborate and has no effect on the H_3BO_3 vapor concentration. The conditions at which to operate an electrostatic precipitator to minimize boron penetration are those lying near the minimum in the curve in Figure 13 where H_3BO_3 vapor takes its lowest values, i.e. $(\text{Na}+\text{K})/(\frac{1}{2}\text{B}+2\text{S})$ greater than about 0.98 and temperature near 490 °F.

An alternative presentation of the relationship of H_3BO_3 vapor concentration to the $(\text{Na}+\text{K})/(\frac{1}{2}\text{B}+2\text{S})$ ratio is shown in Figure 14 for a temperature of 485 °F, near the minimum in the curve of Figure 13. On the left in Figure 14, when the flue gas is deficient in alkali, the orthoboric acid concentration decreases linearly with addition of sodium until the minimum H_3BO_3 is reached, at $(\text{Na}+\text{K})/(\frac{1}{2}\text{B}+2\text{S})$ just slightly above 0.98. Beyond that point, addition of sodium has no effect on the H_3BO_3 vapor concentration. To maintain the lowest possible and most stable boron concentration in the gas leaving the precipitator, one would add enough sodium to keep the alkali to boron-plus-sulfur ratio above the minimum value of 0.98 in the face of normal

fluctuations in Na, K, and B volatilization rates and SO₂ and H₂O concentrations. In the system under consideration the minimum H₃BO₃ mole fraction at 485 °F is predicted by the equilibrium model to be 26.4 mol ppm, corresponding to a boron flow rate of 0.45 lb/h.

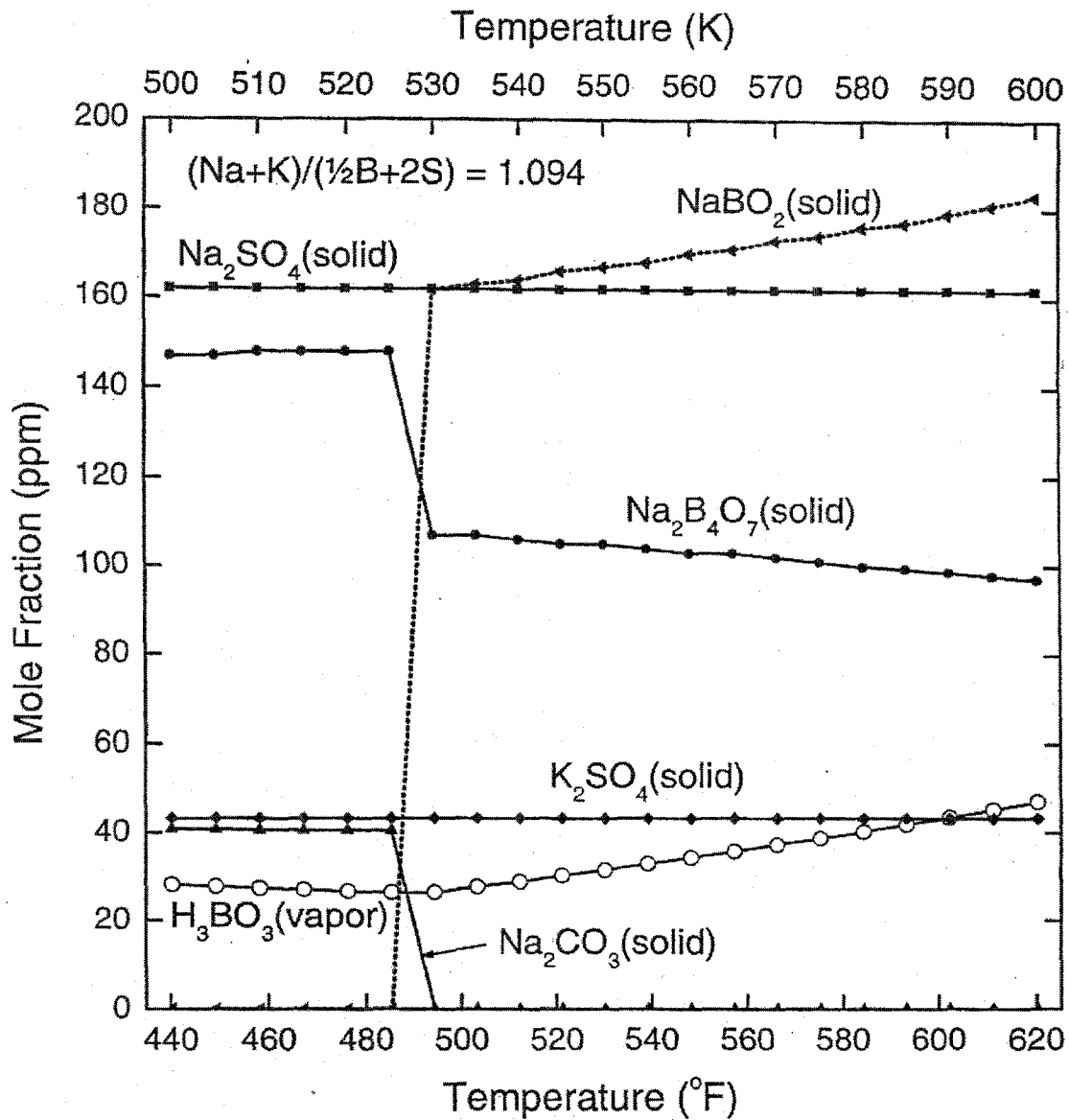


Figure 12. Results of calculations of equilibrium chemical composition in the electrostatic precipitator, similar to those shown in Figures 9, 10, and 11, but with the sodium increased to give an alkali to boron-plus-sulfur ratio of 1.094, the value indicated by chemical analysis of the precipitator dust (Appendix F). Because of the large excess of sodium, the sodium carbonate and sodium metaborate mole fractions are much higher than in Figure 11, but the increase in sodium has no effect on the mole fractions of H₃BO₃ vapor, which are the same as in Figure 11.

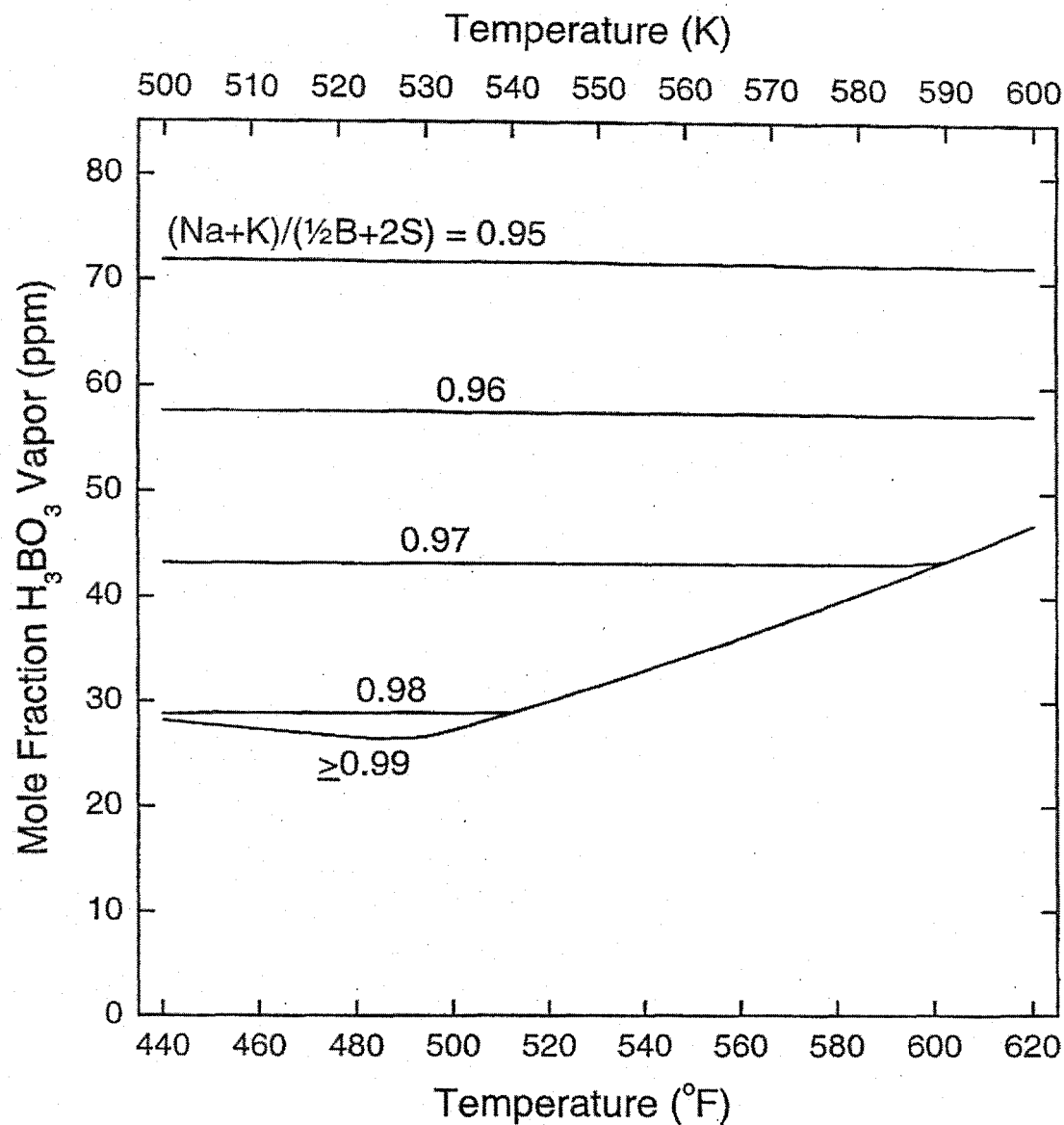


Figure 13. Calculated mole fractions of orthoboric acid (H_3BO_3) vapor as functions of temperature for alkali to boron-plus-sulfur mole ratios of 0.95, 0.96, 0.97, 0.98, and 0.99. The relative amounts of boron, potassium, and sulfur in the system are the same as in Figures 9 to 12. The sodium content was adjusted to vary the alkali to boron-plus-sulfur ratio. The curves for $(Na+K)/(\frac{1}{2}B+2S) = 0.96$ and 0.98 are identical to those for H_3BO_3 in Figures 9 and 10, respectively, but on an expanded scale. The curve for $(Na+K)/(\frac{1}{2}B+2S) \geq 0.99$ is identical to those for H_3BO_3 in Figures 11 and 12.

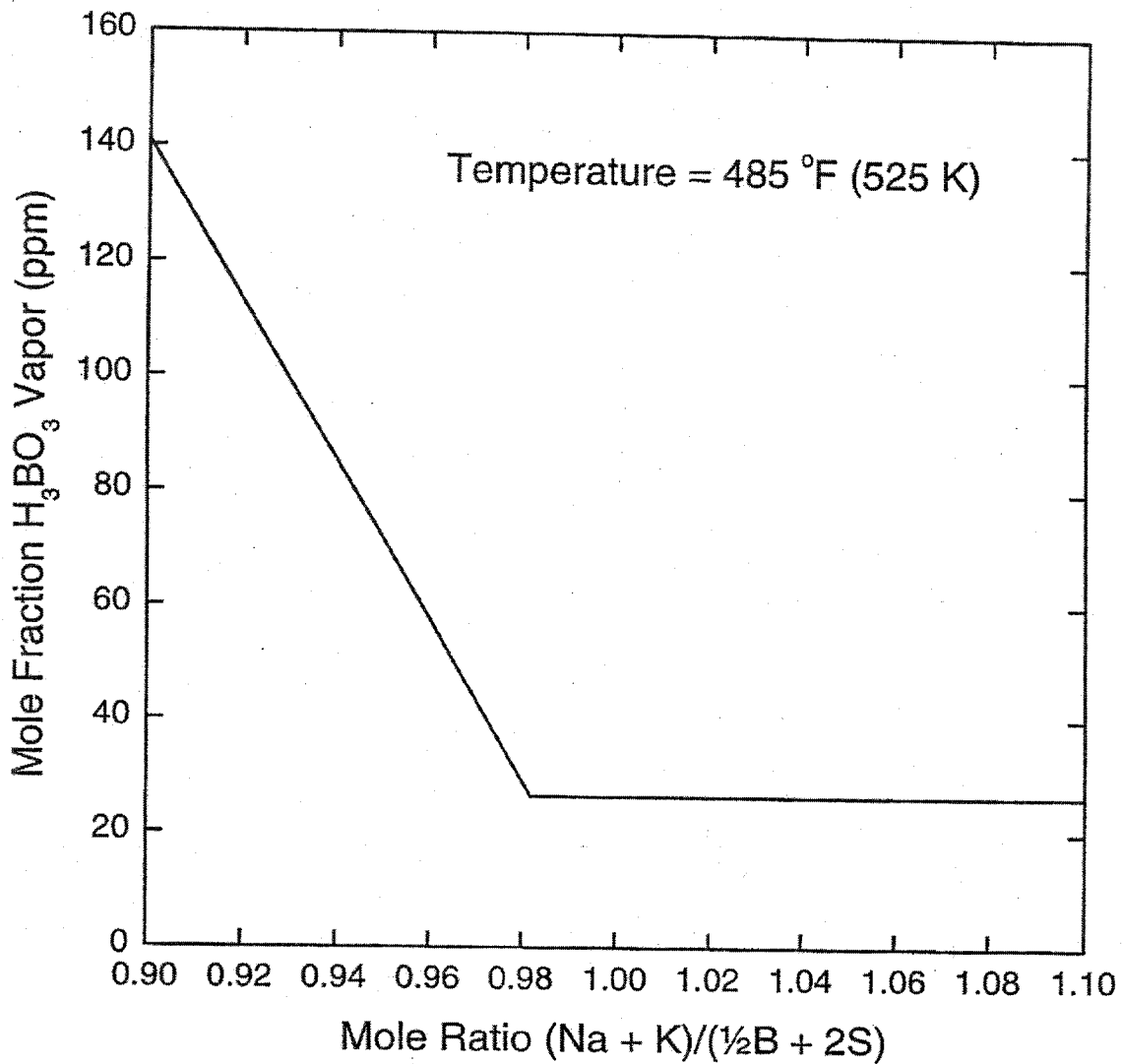


Figure 14. Relationship between orthoboric acid vapor concentration and alkali to boron-plus-sulfur ratio at the precipitator outlet temperature of 485 °F, near the temperature at which the lowest H₃BO₃ vapor concentrations are predicted at equilibrium when excess sodium is present.

DISCUSSION

Temperature

The equilibrium mole fractions of H_3BO_3 vapor for cases having excess sodium over that required to minimize the vapor concentration (curve for $(Na+K)/(\frac{1}{2}B+2S) \geq 0.99$ in Figure 13, in the temperature range from 450 to 490 °F) are converted to boron flow rates and compared with the measurements in Figure 15 (dashed curve). The equilibrium calculation of the orthoboric acid concentration is seen to provide quite a good estimate of the upper limit of the boron flow rates observed at the precipitator outlet and supports the observation that the boron concentration and flow rate decrease slightly with increasing temperature over this range. The minimum in the orthoboric acid concentration occurs at approximately 490 °F. Above this temperature, the trend reverses and the boron concentration increases (see Figure 13). Since the sensitivity of boron to temperature is greater at temperatures above 490 °F than it is below, a temperature near 490 °F, or perhaps slightly higher, is a good choice for the upper limit on gas temperature at the precipitator outlet.

Because the dependence of the orthoboric acid concentration on temperature is apparently rather weak (according to the upper set of measurements in Figure 2 or 15, about a 15% decrease over the range from 454 to 487 °F), it may not be worthwhile to consider adjustment of the precipitator temperature to take advantage of its effect. What is fairly clear, however, is that any reduction in the precipitator outlet temperature below about 480 °F is likely to increase the boron concentration in the exit gas rather than decrease it, the latter being the trend one would expect if the boron vapor concentration were controlled by a simple vapor-liquid or vapor-solid equilibrium.

Sodium Addition

Comparison of the equilibrium calculations with the measurements, plotted as a function of the sodium feed rate to the caustic spray tower, are shown in Figure 16. The predictions of the NASA CEA Code, shown as dashed lines, were derived from calculations of the H_3BO_3 vapor mole fraction versus alkali to boron-plus-sulfur ratio, such as those shown in Figure 14. The temperatures used for the calculations were chosen in the middle of the ranges indicated at the upper right in each figure: 480 and 460 °F for Figures 16a and b, respectively. According to the calculations, which are based on a rough estimate of the total dust flow rate to the electrostatic precipitator, the minimum H_3BO_3 vapor concentration should have been maintained at sodium feed rates down to approximately 5.7 lb/h, where the dashed lines rise steeply on the left. This is a flow rate approximately 3 lb/h lower than the feed rate at the base run condition (8.62 lb/h). However, the predicted steep rise in boron for sodium feed rates below about

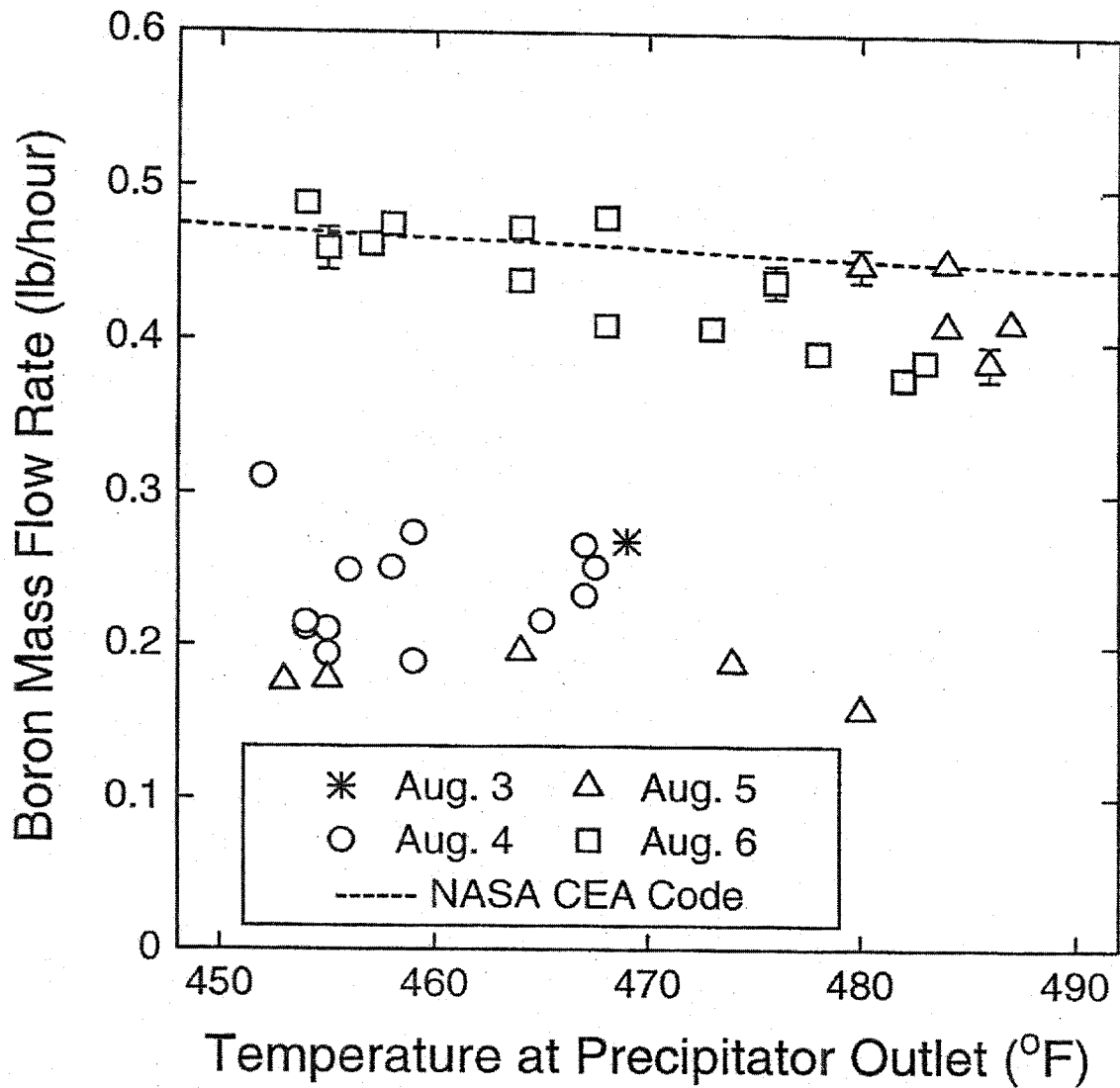


Figure 15. Comparison of the measurements of boron flow rate at the precipitator outlet with the calculations of boron expected at equilibrium using the NASA CEA Code (dashed curve), shown as functions of temperature. The curve is derived from the mole fractions of H_3BO_3 vapor shown for $(Na+K)/(1/2B+2S) \geq 0.99$ in Figure 13.

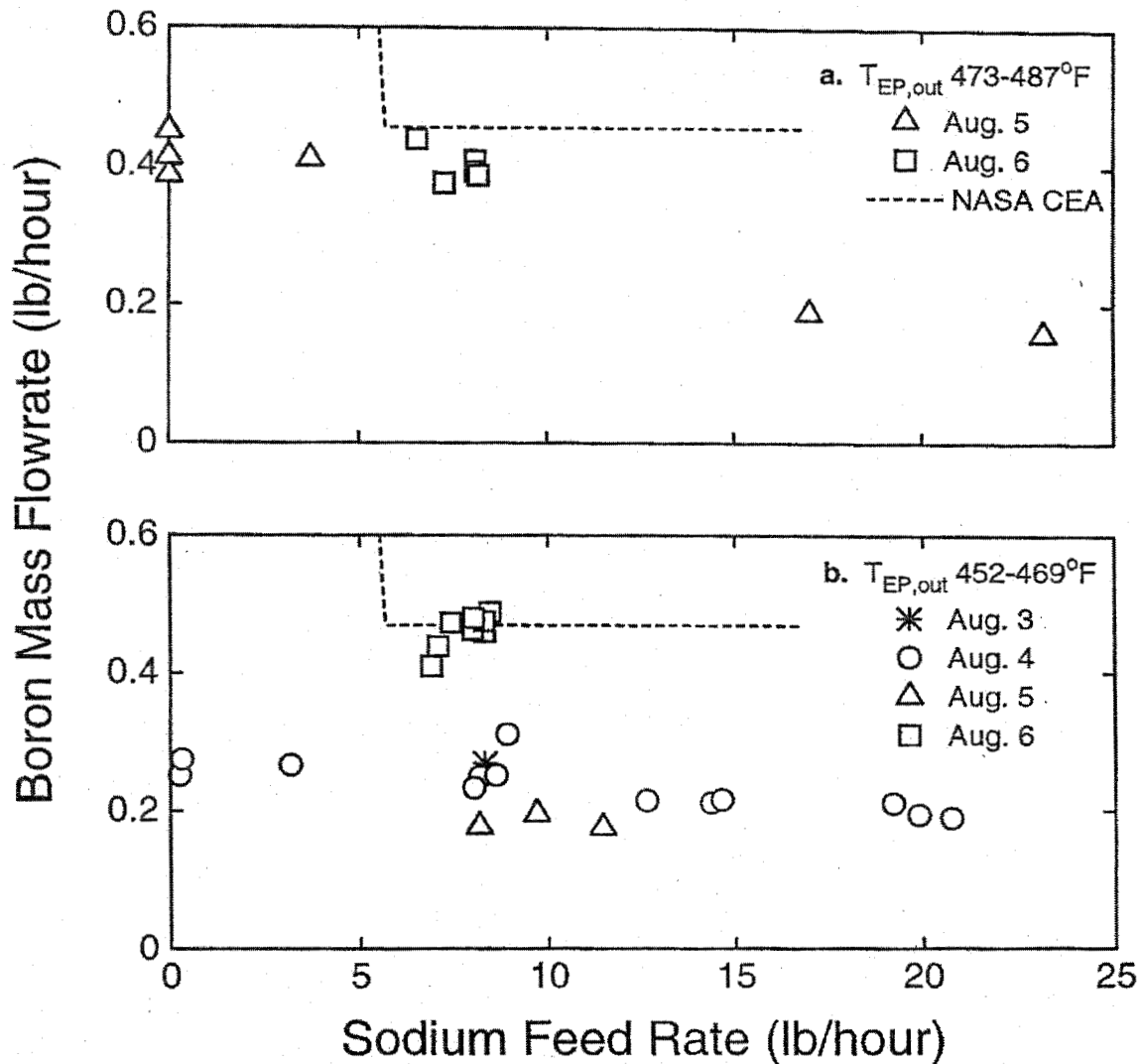


Figure 16. Comparison of the measurements of boron flow rate at the precipitator outlet with the calculations of boron expected at equilibrium using the NASA CEA Code, shown as functions of the sodium feed rate to the caustic spray tower. The equilibrium results (dashed lines) are derived from calculations of H_3BO_3 vapor mole fractions versus the alkali to boron-plus-sulfur ratio, such as those shown in Figure 14. Based on the estimated dust flow rate and its chemical analysis (Appendix F), a sodium feed rate of 5.7 lb/h is predicted to have been required to reduce boron at the precipitator outlet to the lowest achievable level. The measurements do not agree, showing no dramatic increase in boron flow rate even at negligible sodium feed rates.

- a. Calculation for electrostatic precipitator outlet temperature of 480 °F.
- b. Calculation for electrostatic precipitator outlet temperature of 460 °F.

5.7 lb/h is not in agreement with the measurements, which show no such dramatic increase in boron even when the sodium feed rate was negligible. Within each of the groups of data points there are only small changes in the boron flow rate with sodium addition, suggesting that there was already sufficient sodium in the flue gas to convert boron to sodium tetraborate without addition of any caustic soda in the spray tower.

The prediction that 5.7 lb Na/h were needed to achieve the maximum amount of boron capture when, in fact, no sodium may have been needed at all, may be due to our having underestimated the dust collection rate or to the difficulty of obtaining a representative sample of the dust. The composition and concentration of the dust change from the inlet to the outlet of the precipitator as the temperature drops (moving from right to left in Figure 12) and the dust is removed from the gas. This would very likely result in stratification of the composition of dust falling into the hopper, where its composition would continue to evolve according to the local temperature. A more detailed calculation, including the contribution of calcium and magnesium to sulfur capture, would also move the location of the steep rise in boron flow rate in Figures 16a and b farther to the left, to lower sodium feed rates.

In summary, the lack of strong dependence of the boron flow rate on sodium addition suggests that the composition of the system, with or without sodium addition, lies in the region where the H_3BO_3 vapor concentration is independent of the alkali to boron-plus-sulfur ratio, i.e. in the flat region on the right in Figure 14, where $(Na+K)/(\frac{1}{2}B+2S)$ is greater than about 0.98. This does not necessarily mean that sodium addition is unnecessary, because a large margin may be required to allow for fluctuations in boron, sodium, sulfur, potassium, calcium, magnesium, and other elements due to changes in batch composition, furnace conditions, and volatilization and dust carryover rates. For example, a substantial change in the sodium flow rate leaving the furnace was associated with changes in the oxygen-to-natural gas ratio during the tests in August 2000 (Walsh, Johnsen, and Ottesen, 2001). A perhaps unexpected result of the equilibrium calculations is the prediction that the most stable sodium/boron compound under the conditions in the precipitator is sodium tetraborate, which is twice as effective at immobilizing boron as sodium metaborate.

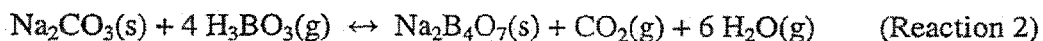
Another piece of evidence that sodium is present in relatively large excess over the minimum required to react with boron is the presence of carbonate in the precipitator dust sample collected under the base case run condition (Appendix F, 3rd line of report). The amount corresponds to 0.0883 moles of carbonate per 100 g of dust. Assuming that this was all present as Na_2CO_3 , it indicates that the excess alkali to boron-plus-sulfur ratio was 0.18, or $(Na+K)/(\frac{1}{2}B+2S) = 1.18$, compared with the value of 1.094 calculated from the sodium and potassium mass fractions in the dust. Based on the carbonate analysis alone, we would conclude that about 5 lb/h of sodium were fed to the caustic spray tower in excess of the amount needed to capture boron.

Atomizing Air Pressure

The apparent lack of sensitivity of the boron flow leaving the precipitator to changes in the atomizing air pressure suggests that the atomizing air pressure could be set at the low end of the range of pressures recommended by the manufacturer of the spray nozzle, to minimize both compressed air consumption and wear of the nozzle. However, the effect of an increase in specific surface area (ft^2/lb) of the sodium hydroxide particles formed when the caustic soda spray droplets dry out would be expected to be similar to the effect of an increase in sodium hydroxide feed rate, i.e. little or no effect as long as sufficient sodium and surface area are present. Therefore, the lack of clear trend in Figures 4a and 4b may simply reflect the fact that sufficient sodium and surface area were present. If the sodium feed rate and $(\text{Na}+\text{K})/(\frac{1}{2}\text{B}+2\text{S})$ ratio are adjusted to minimize caustic soda consumption, particle size and specific surface area may become more critical, so it may then be worthwhile to reexamine the influence of the atomizing air pressure.

Water Vapor

The concentration of H_3BO_3 vapor is increased by addition of quench water and the water in the caustic soda solution. Consider the following reaction, relating Na_2CO_3 , H_3BO_3 , and $\text{Na}_2\text{B}_4\text{O}_7$, in the temperature range where sodium carbonate is stable, below about 485 °F:



Because the concentrations (kmol/m^3) of solids are approximately constant, the solid species in Reaction 2 do not appear in its equilibrium constant,

$$K_2 = \frac{P_{\text{CO}_2} P_{\text{H}_2\text{O}}^6}{P_{\text{H}_3\text{BO}_3}^4} \quad (1)$$

Under conditions of composition and temperature when both Na_2CO_3 and $\text{Na}_2\text{B}_4\text{O}_7$ are present, the H_3BO_3 vapor concentration is independent of the sodium concentration and depends only upon the carbon dioxide and water vapor concentrations (or partial pressures). However, sodium must be within the range required to satisfy the condition that both Na_2CO_3 and $\text{Na}_2\text{B}_4\text{O}_7$ be present, i.e. $(\text{Na}+\text{K})/(\frac{1}{2}\text{B}+2\text{S})$ greater than about 1.0. Equation (1) shows that the H_3BO_3 vapor concentration is expected to increase approximately as the 3/2 power of the water vapor concentration at a fixed temperature. The same dependence of H_3BO_3 on water vapor concentration is expected in the higher temperature regime, above 495 °F, when NaBO_2 and $\text{Na}_2\text{B}_4\text{O}_7$ are the stable solid species, according to Reaction 1. The cumulative effects of changes in temperature and changes in water vapor concentration might make it worthwhile to consider controlling the water

flow rate to the caustic spray tower in order to maintain the electrostatic precipitator outlet temperature in the vicinity of 490 °F.

Collection Efficiency for Sodium

As far as one can tell, by comparison of Figures 1-4 with Figures 5-8, respectively, there is no relationship between the flow rates of boron and sodium leaving the electrostatic precipitator. This is consistent with the passage of boron as orthoboric acid vapor and sodium as solid particles of sodium borates, sodium sulfate, and sodium carbonate. The appearance of sodium in the LIBS spectra at low frequency and high concentration (low concentration of large particles or agglomerates) suggests that the principal mechanism for sodium penetration through the precipitator is reentrainment. Taking the upper limit on the sodium flow rate leaving the precipitator as 0.0011 lb/h, the estimate of 115 lb/h of dust entering the precipitator, and the sodium oxide analysis of the dust (Appendix F), indicates a collection efficiency for sodium greater than 99.996%. Sodium and boron are expected to occur together in the most abundant components of the dust under the conditions investigated, as $\text{Na}_2\text{B}_4\text{O}_7$. Therefore, we expect the collection efficiency for particulate boron to be nearly the same as that for particulate sodium. This observation provides additional support for the view that most of the boron leaving the precipitator is in the form of vapor.

According to the equilibrium calculations, the dust undergoes a marked change in composition over the temperature interval from 485 to 495 °F, when the form of excess sodium changes from sodium carbonate to sodium metaborate, as shown in Figure 12. It is possible that a change in particle size distribution, dust cake resistivity, or other property influencing collection efficiency accompanies this change in composition. There is a hint of such an effect in the large standard deviations of the sodium measurements near the precipitator outlet temperature of 485 °F in Figure 6, but the collection efficiency for sodium was still quite high under this condition.

Remaining Questions

An effect remaining to be explained is the marked change in boron flow rate at 14:00 hours on August 5 (Figure 1) and the resulting separation of the data into two non-overlapping groups (Figures 2 and 3b). According to the results of the equilibrium calculations, large changes in H_3BO_3 vapor concentration are only possible when the alkali to boron-plus-sulfur, $(\text{Na}+\text{K})/(\frac{1}{2}\text{B}+2\text{S})$, is less than about 0.98 (Figures 13 and 14), but the measurements in Figures 3 and 16 indicate that sodium was present in excess, because changing the sodium feed rate had little effect. There is, at least at present, no satisfactory explanation for the separation of the data into the two distinct groups. The warning to be taken from this is that, though the measurements and equilibrium calculations have provided some useful insight into the behavior of the boron/sodium/potassium/sulfur system, we still have more to learn about volatilization in borosilicate glass melting, the exhaust treatment system, and the technique of laser-induced breakdown spectroscopy.

SUMMARY, CONCLUSIONS, AND RECOMMENDATIONS

Summary and Conclusions

Boron and sodium concentrations in the flue gas from a borosilicate glass melting furnace were measured downstream from the flue gas treatment system. The treatment system consisted of water addition for control of temperature, a caustic soda spray tower to promote conversion of boric acid vapor to solid sodium borates, and an electrostatic precipitator for particulate removal. The objective of the work was to determine the dependence of boron and sodium penetration through the precipitator on the concentration and flow rate of caustic soda to the spray tower and the pressure of its atomizing air. The measurement technique was laser-induced breakdown spectroscopy (LIBS), whose principal advantage over other techniques in this application is rapid time response and rapid turnaround of results. It was possible for the team performing the experiments to see immediately the effects of changes in the test conditions on the boron concentration. Mass flow rates of boron and sodium were calculated by taking the product of the concentrations determined using LIBS and measurements of the flue gas flow rate.

Interpretation of the results was facilitated by comparison with predictions of the chemical composition of the system at equilibrium using the NASA Chemical Equilibrium with Applications (CEA) Code. The most important of the stable compounds, under the conditions of temperature, pressure, and elemental composition of the flow in the precipitator were predicted to be potassium sulfate, K_2SO_4 , sodium sulfate, Na_2SO_4 , sodium tetraborate, $Na_2B_4O_7$, sodium metaborate, $NaBO_2$, orthoboric acid, H_3BO_3 , and sodium carbonate, Na_2CO_3 . All are solids except orthoboric acid, H_3BO_3 , which is present as vapor and passes through the precipitator. The results of the calculations can be summarized as follows: At equilibrium under the conditions investigated, SO_2 is completely converted to potassium and sodium sulfates. The remaining sodium reacts first with boron to form sodium tetraborate. Below about 485 °F, any sodium in excess of the maximum amount that will react with boron forms sodium carbonate. Above about 495 °F, the excess sodium reacts with sodium tetraborate to form sodium metaborate. Regardless of how much excess sodium is provided, conversion of orthoboric acid vapor to solid sodium borates is not complete.

Combining the information provided by the equilibrium calculations with the actual mole fractions of the elements in the dust catch suggested that a useful parameter for characterization of the state of the system with respect to conversion of orthoboric acid to sodium tetraborate is the molar ratio, $(Na+K)/(1/2B+2S)$, in the precipitator. The construction of this ratio was based on the observation from the equilibrium calculations that the most stable compounds of K, Na, S, and B over the range of compositions